Circulation Research
JOURNAL OF THE AMERICAN HEART ASSOCIATION

Plasma MicroRNA Profiling Reveals Loss of Endothelial MiR-126 and Other MicroRNAs in Type 2 Diabetes

Anna Zampetaki, Stefan Kiechl, Ignat Drozdov, Peter Willeit, Ursula Mayr, Marianna Prokopi, Agnes Mayr, Siegfried Weger, Friedrich Oberhollenzer, Enzo Bonora, Ajay Shah, Johann Willeit and Manuel Mayr

Circ. Res. published online Jul 22, 2010;
DOI: 10.1161/CIRCRESAHA.110.226357
Circulation Research is published by the American Heart Association. 7272 Greenville Avenue, Dallas, TX 72514
 Print ISSN: 0009-7330. Online ISSN: 1524-4571

Plasma MicroRNA Profiling Reveals Loss of Endothelial MiR-126 and Other MicroRNAs in Type 2 Diabetes

Anna Zampetaki,* Stefan Kiechl,* Ignat Drozdov, Peter Willeit, Ursula Mayr, Marianna Prokopi, Agnes Mayr, Siegfried Weger, Friedrich Oberhollenzer, Enzo Bonora, Ajay Shah, Johann Willeit, Manuel Mayr

Rationale: **MicroRNAs (miRNAs) have been implicated in the epigenetic regulation of key metabolic, inflammatory, and antiangiogenic pathways in type 2 diabetes (DM) and may contribute to common disease complications.**

Objective: **In this study, we explore plasma miRNA profiles in patients with DM.**

Methods and Results: **Total RNA was extracted from plasma samples of the prospective population-based Bruneck study. A total of 13 candidate miRNAs identified by microarray screening and miRNA network inference were quantified by quantitative PCR in all diabetic patients of the Bruneck study and age- and sex-matched controls (1995 evaluation, n=80 each). Quantitative PCR assessment revealed lower plasma levels of miR-20b, miR-21, miR-24, miR-15a, miR-126, miR-191, miR-197, miR-223, miR-320, and miR-486 in prevalent DM, but a modest increase of miR-28-3p. Findings emerged as robust in multivariable analysis and were independent of the standardization procedure applied. For endothelial miR-126, results were confirmed in the entire Bruneck cohort (n=822) in univariate (odds ratio [95% confidence interval], 0.38 [0.26 to 0.55]; P=2.72ptimes]10^{-7}) and multivariate analyses (0.57 [0.37 to 0.86]; P=0.0082). Importantly, reduced miR-15a, miR-29b, miR-126, miR-223, and elevated miR-28-3p levels antedated the manifestation of disease. Most differences in miRNA levels were replicated in plasma obtained from hyperglycemic Lep^{ob} mice. High glucose concentrations reduced the miR-126 content of endothelial apoptotic bodies. Similarly in patients with DM, the reduction of miR-126 was confined to circulating vesicles in plasma.**

Conclusions: **We reveal a plasma miRNA signature for DM that includes loss of endothelial miR-126. These findings might explain the impaired peripheral angiogenic signaling in patients with DM. (*Circ Res*. 2010;107:00-00.)**

Key Words: diabetes mellitus ■ microRNA ■ vascular endothelium

MicroRNAs (miRNAs) are a class of small noncoding RNAs that function as translational repressors. They bind through canonical base pairing to a complementary site in the 3′ untranslated region of their target mRNAs and can direct the degradation or translational repression of these transcripts.[1–2] MiRNAs have been shown to play important roles in development, stress responses, angiogenesis, and oncogenesis.[3–4] Accumulating evidence also points to an important role of miRNAs in the cardiovascular system.[4–5] For example, miRNAs modulate endothelial cell function and regulate their inflammatory response and angiogenic potential.[6–7]

Recently, Mitchell et al highlighted the presence of miRNAs in plasma.[8] These plasma miRNAs are not cell-associated, but packaged in microvesicles that protect them from endogenous RNase activity. Interestingly, plasma miRNAs can display unique expression profiles: specific tumor miRNAs were identified in cancer patients,[9] whereas tissue-derived miRNAs constitute a marker for injury.[10–11] In cardiovascular diseases, circulating miRNAs have been investigated in sepsis, myocardial injury, coronary artery disease, and heart failure.[12–15] Type 2 diabetes mellitus (DM) is one of the major risk factors of cardiovascular disease leading to endothelial dysfunction and micro- and macrovascular complications.[16–17] However, a systematic analysis of plasma miRNAs in DM has not yet been performed.

The present study is the first to reveal a plasma miRNA signature for DM in a large population-based cohort. Our findings may provide new insights into the pathophysiology of DM and the manifestation of its vascular complications.

Original received June 16, 2010; revision received July 11, 2010; accepted July 13, 2010. In June 2010, the average time from submission to first decision for all original research papers submitted to *Circulation Research* was 14.5 days.

From the King's College London British Heart Foundation Centre (A.Z., I.D., U.M., M.P., A.S., M.M.) and Centre for Bioinformatics-School of Physical Sciences and Engineering (I.D.), King's College London, United Kingdom; Department of Neurology (S.K., P.W., J.W.), Medical University Innsbruck, Austria; Department of Public Health and Primary Care (P.W.), University of Cambridge, United Kingdom; Department of Laboratory Medicine and Department of Internal Medicine (A.M., S.W., F.O.), Bruneck Hospital, Italy; and Division of Endocrinology and Metabolic Diseases (E.B.), University Hospital of Verona, Italy.

This manuscript was sent to Ali J. Marian, Consulting Editor, for review by expert referees, editorial decision, and final disposition.

*Both authors contributed equally to this work.

Correspondence to Dr Manuel Mayr, King's British Heart Foundation Centre, King's College London, 125 Coldharbour Lane, London SE5 9NU, United Kingdom. E-mail manuel.mayr@kcl.ac.uk

Circulation Research **is available at http://circres.ahajournals.org** **DOI: 10.1161/CIRCRESAHA.110.226357**

Non-standard Abbreviations and Acronyms

CI	confidence interval
CLR	context likelihood of relatedness
DM	type 2 diabetes
HUVEC	human umbilical vein endothelial cell
Lep^{ob}	Leptin obese
miRNA	microRNA
PCA	principal component analysis
PCC	Pearson correlation coefficient
qPCR	quantitative PCR
VEGF	vascular endothelial growth factor

Methods

An expanded Methods section is available in the Online Data Supplement at http://circres.ahajournals.org.

Study Subjects

The Bruneck study is a prospective population-based survey initially designed to investigate the epidemiology and pathogenesis of atherosclerosis and later extended to study all major human diseases including DM.[18–20] At the baseline evaluation in 1990, the study population was recruited as a sex- and age-stratified random sample of all inhabitants of Bruneck (Bolzano Province, Italy) 40 to 79 years old. During 1990 and the re-evaluation in 1995 (the first five-year period), a subgroup of 63 individuals died or moved away. In the remaining population follow-up was 96.5% complete (n=822). RNA extraction was performed from blood specimens collected as part of the 1995 follow-up in 822 individuals. Follow-up in 2000 and 2005 was 100% complete for clinical end points and >90% complete for repeated laboratory examinations. Assessment of the ankle-brachial index and incident peripheral artery disease is described in detail in the Online Data Supplement. The Bruneck population is highly representative of the general community and shows characteristics similar to those of other Western countries. The mean age was 62.9 years, 49.9% were women and the prevalence of DM was 9.7%. Their clinical characteristics are summarized in Online Table I. The protocols of the Bruneck study were approved by the appropriate Ethics Committees, and all study subjects gave their written informed consent before entering the study.

Ascertainment of DM

Presence of DM was established according to World Health Organization criteria, ie, when fasting glucose was ≥7 mmol/L (126 mg/dL) or when the 2-hour oral glucose tolerance test glucose level was ≥11.1 mmol/L (200 mg/dL) or when the subjects had a clinical diagnosis of the disease. Self-reported DM status was obligatorily confirmed by reviewing the medical records of the subject's general practitioners and files of the Bruneck Hospital (for details, see the Online Data Supplement).

MiRNA Expression Profile

RNA extraction was performed using the miRNeasy kit (Qiagen) from blood specimens collected as part of the 1995 follow-up in 822 individuals. MiRNAs were reverse-transcribed using the Megaplex Primer Pools (Human Pools A v2.1 and B v2.0), and expression was screened using TaqMan miRNA Arrays A and B (all from Applied Biosystems). TaqMan miRNA assays were used to determine the expression of individual miRNAs. Additional details are provided in the Online Data Supplement.

Sampling Strategy and Statistical Analysis

For the initial microarray screening, 2 pools of plasma obtained from 5 individuals with DM each (randomly selected from the 80 patients with DM in the Bruneck study) and 6 pools of plasma obtained from controls identical in age, sex, risk factor profile (low-density lipoprotein, smoking, hypertension), and atherosclerosis status were used. Quantitative (q)PCR was performed for the 13 miRNAs that showed correlation with DM. TaqMan assays were run in duplicates. Two groups of patients were assessed: group 1, all subjects with manifest DM in the Bruneck cohort (1995, n=80); group 2 to 19, patients who developed DM between 1995 and 2005 (incident DM). Eighty and 19 matched individuals identical for age and sex with fasting glucose levels of <6.1 mmol/L (110 mg/dL), 2-hour glucose of <7.7 mmol/L (140 mg/dL), and no history of DM served as controls. In the case of several suitable matches, all were numbered in ascending order and one was selected by means of a computer-based random number generator. Finally, miR-126 was measured in the entire population of 822 individuals. For the lack of generally accepted standards all qPCR data were analyzed as unadjusted Ct values and standardized to both miR-454 and RNU6b, a small nuclear RNA, which fulfilled the following criteria: detectable in all samples, low dispersion of expression levels and null association with DM status. Moreover, the miR-454 expression profile showed little association with other miRNAs and positioned outside the coexpression modules of the complex miRNA network in plasma (Figure 1). Data were analyzed using SPSS version 15.0 and STATA version 10 software packages. Continuous variables were presented as means±SD or median (interquartile range) and dichotomous variables as numbers and percentages. Fold changes of individual miRNAs were calculated for each pair of matched (pre)diabetic cases and controls by dividing the standardized expression levels of the miRNAs. The median of fold changes is presented in Figure 1. Differences in miRNA levels between subjects with prevalent or

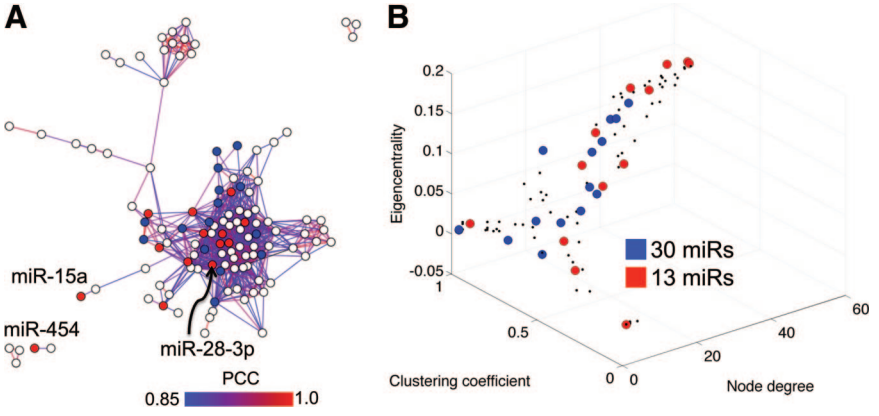

Figure 1. MiRNA coexpression network and miRNA topology values. A, Weighted and undirected miRNA coexpression network. Nodes correspond to miRNAs and edges (links) indicate similarity in miRNA expression, as measured by the PCC. Strength of similarity is indicated by a **red-blue edge color gradient**. At PCC values of >0.85, the coexpression network consisted of 120 miRNAs and 1020 coexpression. **B,** Relationships of node degrees (number of coexpressing pairs for each miRNA), clustering coefficients (likelihood of miRNA sharing a large number of neighbors), and eigenvector centralities (relative contribution of miRNA to stability of the network) for 120 miRNAs. There were 30 differentially expressed miRNAs **(blue)**, of which 13 **(red)** occupied locations important to maintenance of the overall network structure.

incident DM and corresponding groups of matched controls were analyzed using the nonparametric Wilcoxon test for related samples with computation of exact probability values. To account for the potential confounding effects of lifestyle features and other variables related to DM and to analyze for interactions, we additionally performed logistic regression analyses for matched data that include $\log_e$-transformed expression levels of miRNAs (1 per model) and the following variables: social status, family history of DM, body mass index, waist-to-hip ratio, smoking status, alcohol consumption (g/d), physical activity (sports index), and high-sensitivity C-reactive protein. Details on model construction were described by Hosmer and Lemeshow.[21] First-order interactions between miRNAs and the above variables, as well as age and sex, were calculated by inclusion of appropriate interaction terms. None of these terms achieved statistical significance. Cox proportional hazard models were used to assess the predictive value of miR-126 for new-onset peripheral artery disease. Participants who experienced an outcome event were censored with respect to subsequent follow-up. The proportional hazard assumption was confirmed for miR-126 by testing the interaction of miR-126 with a function of survival time (Cox models with time-dependent covariates). A total of 37 subjects with symptomatic peripheral artery disease at baseline were excluded, leaving 785 subjects for this analysis. The potential association between miR-126 and low ankle–brachial index was analyzed by means of logistic regression analysis. This analysis was fit to the entire study population. Differences in miR-126 between categories of glucose tolerance were compared with General Linear Models. All probability values presented are 2-sided.

MiRNA Coexpression Network Inference and Analysis

Network inference algorithms were applied to evaluate global expression properties of miRNAs in DM. Similarity in miRNA expression profiles was interrogated using either Pearson correlation coefficients (PCCs) or context likelihood of relatedness (CLR) between all possible miRNA pairs.[22] Pairs that maintained dependence above a predefined threshold were represented in the form of an undirected weighted network, where nodes correspond to miRNAs and links (edges). Although PCC is a way to measure linear relationships between features (miRNAs), CLR relies on a mutual information metric and does not assume linearity,[23–24] thus possessing some flexibility to detect biological relationships that may otherwise be missed. PCC was used to detect clusters of similarly expressed miRNAs from a high throughput space of expression arrays, whereas CLR was used to identify all nonrandomly associated qPCR-validated miRNA profiles. Although PCC and CLR sometimes yield similar results, CLR was chosen for qPCR-validated miRNAs because it is more sensitive to nonlinear dynamics of miRNA expression than PCC and significantly outperforms other network inference methods (eg, ARACNE) in identifying biologically meaningful relationships.[25–26] The PCC threshold was set to a point where miRNA coexpression network began to acquire a scale-free architecture, which is a characteristic of most real-world networks, including, biological ones.[27] To ensure reproducibility, the 30 differentially expressed miRNAs were evaluated by assessing their network properties,[28] rather than the magnitude of over- or underexpression. The CLR threshold was chosen such that all 13 miRNAs could be represented in the network while retaining the smallest possible number of links between them.

Topological Analysis

During prescreening, miRNAs were studied by virtue of their topology in the global miRNA coexpression network, as well as individual over- or underexpression. For each miRNA, topological parameters including node degree, clustering coefficient, and eigenvector centrality were systematically calculated. Node degree is defined as the total number of edges that are connected to a given miRNA. Clustering coefficient is the degree to which miRNAs tend to cluster together. Eigenvector centrality is a measure of miRNA importance, such that a particular miRNA receives a greater value if it is strongly correlated with other miRNAs that are themselves central within the network.

Endothelial Cell Culture

Human umbilical vein endothelial cells (HUVECs) were purchased from Cambrex and cultured on gelatin-coated flasks in M199 medium supplemented with 1 ng/mL endothelial cell growth factor (Sigma), 3 μg/mL endothelial growth supplement from bovine neural tissue (Sigma), 10 U/mL heparin, 1.25 μg/mL thymidine, 5% FBS, 100 μg/mL penicillin and streptomycin as described previously.[29,30] HUVECs exposed to high glucose (25 mmol/L) were cultured in complete medium for 6 days. As a control, HUVECs were cultured in complete medium (5 mmol/L glucose) supplemented with mannitol, to exclude effects of osmotic stress. On day 5, cells were counted and an equal number of cells was seeded on T75 flasks and incubated for an additional day.

Isolation of Vesicles

Vesicles were isolated as described previously.[31] In brief, HUVECs were deprived of serum and growth factors for 24 hours before the conditioned medium was harvested and the cells were lysed in QIAzol reagent. The cellular lysates were stored at −20°C for miRNA expression analysis. The conditioned medium was first precleared by centrifugation for 10 minutes at 800*g* to remove any floating cells. Then, endothelial particles (apoptotic bodies) were isolated by centrifugation at 10 600 rpm for 20 minutes. Subsequently, an additional centrifugation step was performed at 20 500 rpm for 2 hours to isolate small microparticle (size, <1 μm) shedding from endothelial cells. Identical centrifugation steps were performed to obtain vesicles from plasma. The pelleted vesicles were resuspended in PBS and stored at −80°C. Total RNA was extracted using the miRNeasy kit as described above. RNA was quantified using the NanoDrop spectrophotometer and 20 ng of total RNA were used for reverse transcription.

Results

Comprehensive MiRNA Profiling

For the initial screening, Human TaqMan miRNA arrays (CardA v2.1 and CardB v2.0, Applied Biosystems) covering 754 small noncoding RNAs were applied to 8 pooled samples, 2 consisting of subjects with DM, and 6 of appropriate controls (see methods). Of the 148 miRNAs with Ct values of <36, 130 miRNAs were detected using fluidic Card A and therefore all further analysis focused on this data set, resulting in the identification of 30 differentially expressed plasma miRNAs in patients with DM (Online Table II).

MiRNA Network Analysis

MiRNA pairs with high correlation values (PCC >0.85) were represented in the form of an undirected and weighted network. At this threshold, the network was dominated by a small number of hubs that linked with many loosely connected nodes, a property of many biological networks (Online Figure I). The miRNA network consisted of 120 miRNAs (nodes) and 1020 coexpression links (edges) (Online Table II). The 30 differentially expressed miRNAs were sampled by virtue of their localization in the miRNA coexpression network as marker selection using network topology is more reproducible than assessment of individual over- or underexpression.[28] Within the network, the 30 differentially expressed miRNAs were topologically central (Online Figure II; Online Table III). 13 of the 30 differentially expressed miRNAs that displayed extreme spectra of node degrees, clustering coefficients, and eigenvector centrality values were

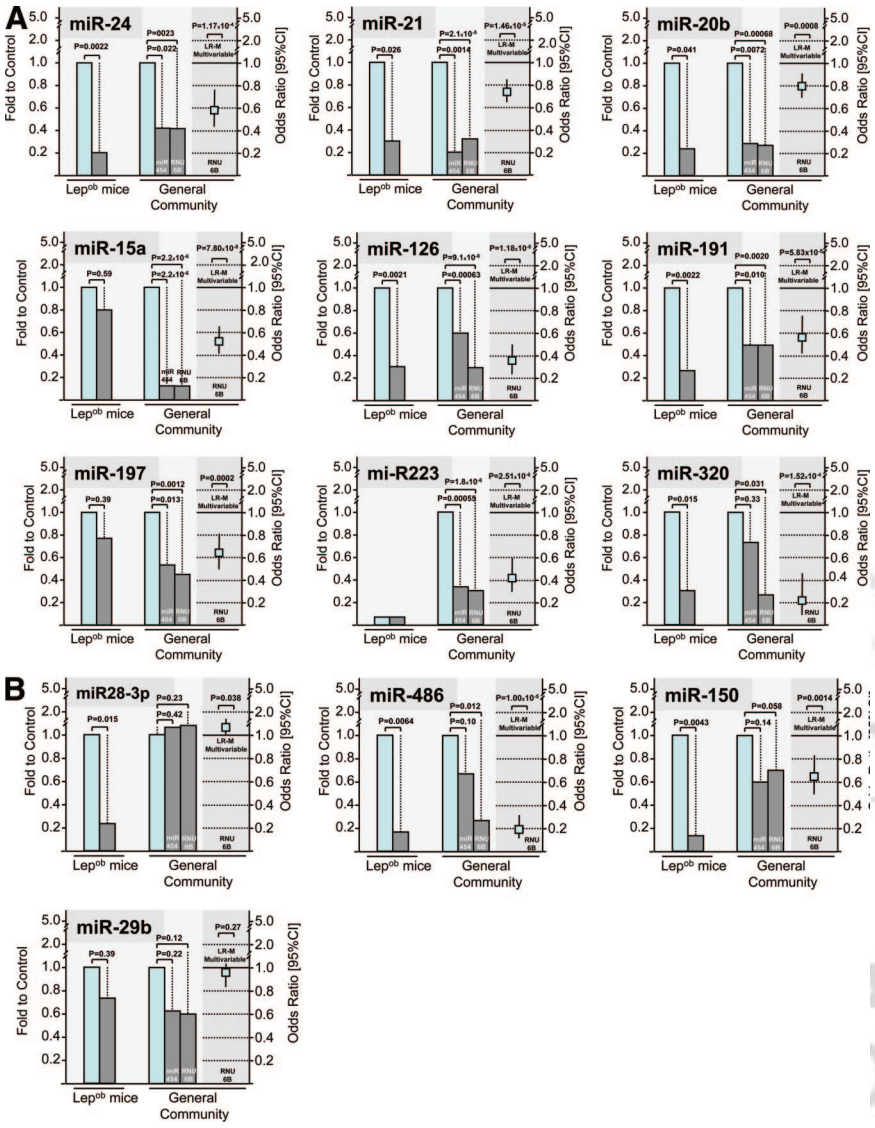

Figure 2. Association of plasma miRNAs with manifest DM. Thirteen plasma miRNAs were quantified by qPCR in patients with prevalent DM and matched controls (n=80 each). **Bars in the center of each graph** represent fold changes of plasma miRNA levels between diabetic patients and controls. **Bars on the left** provide a comparison (fold changes) between plasma obtained from hyperglycemic Lep^{ob} and control mice. **Squares and lines on the right** represent odds ratios (95% CIs) derived from multivariable logistic regression analyses for matched data (human studies). Probability values were from the nonparametric Wilcoxon test for related samples (human studies, center) and Mann–Whitney *U* test for unrelated samples (animal studies), and from multivariable logistic regression analyses for matched data (human studies).

selected (Figure 1B). MiR-454 was the only miRNA that showed no association with the expression of other miRNAs and was positioned outside all network modules (Figure 1A). Thus, it was chosen as an additional normalization control.

Validation by qPCR

The 13 topologically unique miRNAs were further quantified by qPCR. All patients with manifest DM at the time of the 1995 evaluation (n=80) were compared to age- and sex-matched controls (Online Table I). Plasma levels of miR-24, miR-21, miR-20b, miR-15a, miR-126, miR-191, miR-197, miR-223, miR-320, miR-486, miR-150, and miR-29b were lower in diabetic subjects, whereas miR-28-3p tended to be higher (Figure 2). Findings were consistent for expression levels standardized to either miR-454 or RNU6b (Figure 2) and for nonstandardized miRNA levels (data not shown). Nine miRNAs standardized to RNU6b showed significant differences between patients with DM and controls, and 4 remained significant after accounting for the multiple comparisons performed (Bonferroni probability value <0.000133), including endothelial miR-126. Bonferroni correction, however, is overly conservative in this setting because individual miRNAs are not independent of each other but extensively correlated. In multivariate analyses, all miRNAs except miR-29b were significantly associated with manifest DM. Eleven showed an inverse relationship and miR-28-3p a positive one. Findings for miRNAs standardized to miR-454 are summarized in Figure 2 and were similar in diabetic patients with or without drug treatment (mainly sulfonylureas). In another run, miR-126 was quantified in the entire Bruneck cohort (n=822) and standardized against miR-454. In logistic regression analyses, miR-126 emerged again as a significant predictor of manifest DM (odds ratio [95% confidence interval {CI}] for a 1-SD unit decrease of $\log_e$-transformed expression level of miR-126, 2.23 [1.69 to 2.96]; $P=2.28\times10^{-8}$), and this association persisted in a multivariable model (odds ratio [95% CI], 1.64 [1.19 to 2.28]; $P=0.0027$). Moreover, there was a gradual decrease in plasma levels of miR-126 across categories of normal glucose tolerance (n=580), impaired fasting glucose/impaired glucose tolerance (n=162) and manifest DM (n=80) (Figure 3). As expected, levels of miRNAs were inversely correlated with

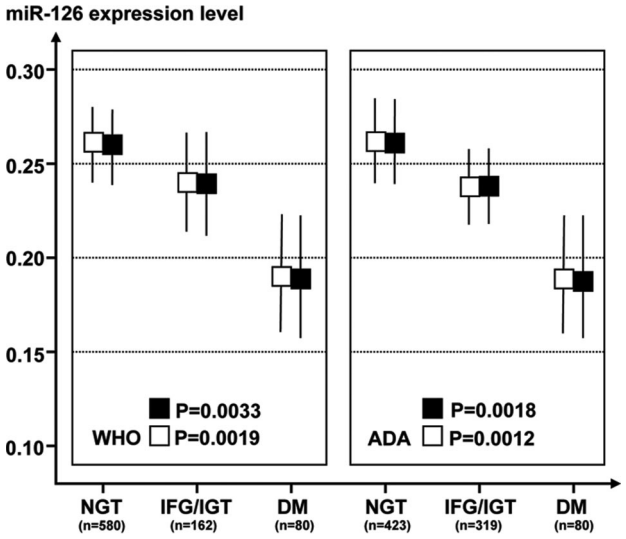

Figure 3. Plasma levels of miR-126 across categories of normal glucose tolerance (NGT), impaired fasting glucose/impaired glucose tolerance (IFG/IGT), and manifest DM. **Squares and lines** indicate adjusted geometric means and 95% CIs (**white squares,** values adjusted for age and sex; **black squares,** values adjusted for age, sex, social status, family history of DM, body mass index, waist-to-hip ratio, smoking status, alcohol consumption (g/d), physical activity (sports index), and high-sensitivity C-reactive protein). This analysis was performed in the entire study population (n=822). Differences in miR-126 between categories of NGT, IFG/IGT and DM were compared with General Linear Models and probability values are for trend. World Health Organization definition of categories: normal glucose tolerance (fasting glucose, <110 mg/dL; 2-hour glucose, <140 mg/dL), impaired fasting glucose/impaired glucose tolerance (110 mg/dL≤fasting glucose<126 mg/dL, 140 mg/dL≤2-hour glucose<200 mg/dL) and manifest DM. American Diabetes Association definition of categories: normal glucose tolerance (fasting glucose, <100 mg/dL; 2-hour glucose, <140 mg/dL), impaired fasting glucose/impaired glucose tolerance (100 mg/dL≤fasting glucose<126 mg/dL, 140 mg/dL≤2-hour glucose<200 mg/dL) and manifest DM.

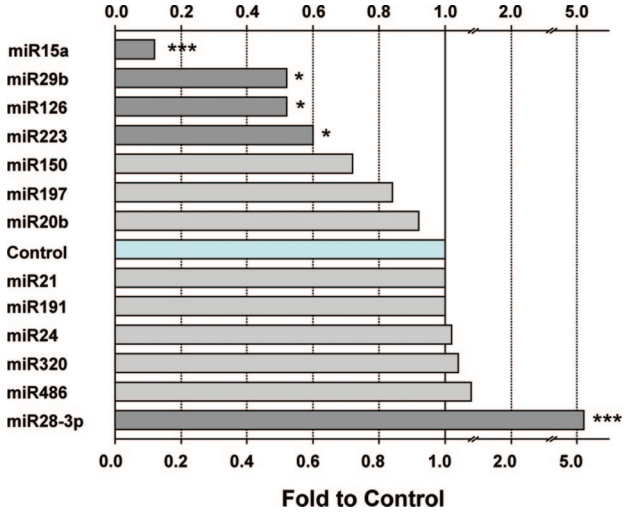

Figure 4. Association of plasma miRNAs with incident DM. Thirteen plasma miRNAs were quantified by qPCR in patients who developed DM over a 10-year observation period and matched controls. Probability values were derived from the nonparametric Wilcoxon test for related samples. *P<0.05, ***P<0.001.

fasting glucose levels in both patients with DM, as well as control subjects (r≈−0.191 to −0.335, P<0.05 each except miR-29b and miR-320) and less consistently with 2-hour glucose levels (r=−0.091 to −0.239) and HbA1c concentrations (r=−0.093 to −0.312). Most of the miRNA changes observed in DM could independently be replicated in plasma samples of 8 to 12 week old hyperglycemic Lep^{ob} mice (Figure 2).

Incident DM

Importantly, several miRNAs were already altered before manifestation of DM. A total of 19 subjects, who were normoglycemic in 1995, developed DM over the 10-year follow-up period (1995 to 2005 mean interval until diagnosis of DM 79.2 months). Baseline levels of miR-15a, miR-29b, miR-126, and miR-223 were significantly lower in these subjects, whereas miR-28-3p was higher compared to matched controls (Figure 4).

MiRNA Networks As biomarkers in DM

To determine whether miRNAs can correctly distinguish individuals with prevalent or incident DM from healthy controls, we reduced miRNA expression to principal components (PC). Interestingly, 91/99 (92%) controls and 56/80 (70%) DM cases were correctly classified using expression profiles of 5 most significant miRNAs (miR-15a, miR-126, miR-320, miR-223, miR-28-3p) (Figure 5). The 24 DM cases that were classified as normal subjects had significantly lower levels of fasting glucose (mean± SD, 120.0±28.6 mg/dL versus 147.2±55.0 mg/dL, P=0.005) and HbA1c (mean± SD, 6.03±0.75% versus 6.66±1.54%, P=0.016) and represent a selection of patients with well-controlled DM. Importantly, using this model 10/19 (52%) of normoglycemic subjects that developed DM over the 10-year follow-up period were already classified as diabetics. Inclusion of additional miRNAs into the classification did not improve model performance (Figure 5B). Thus, these 5 miRNA can be considered as minimal requirement for classification using a miRNA signature. Further support to the putative value of miRNAs as diagnostic tools in DM was provided by the inference of miRNA relevance network (Online Figure III).

MiRNA-126 in DM

Among the miRNAs most consistently associated with DM was miR-126. This miRNA has previously been shown to be highly enriched in endothelial cells and endothelial apoptotic bodies and to govern the maintenance of vascular integrity, angiogenesis, and wound repair.[34–35] To determine whether hyperglycemia affects miR-126 release from endothelial cells, miRNA levels of shedding endothelial particles (apoptotic bodies) and microparticles derived under normal (5 mmol/L) and high (25 mmol/L) glucose concentrations were compared. Whereas cellular miRNA concentrations remained unaltered, high glucose significantly reduced the miR-126 content in endothelial apoptotic bodies (Figure 6A). Shedding of other miRNAs except miR-24 was not affected (Online Figure IV). Consistent with these in vitro experiments, the reduction in miR-126 levels in patients with DM was confined to the particulate fraction in plasma (Figure 6B). Finally, evidence from our population cohort suggests that loss of miR-126 in plasma correlates with

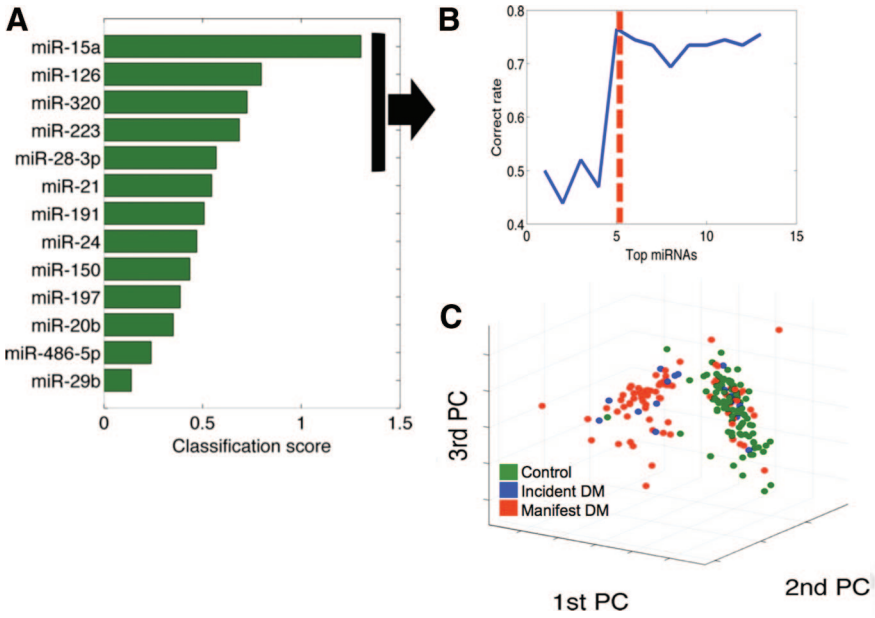

Figure 5. Classification, PCA, and network properties. A, Classification efficiency of 13 miRNAs across control subjects (n=99), patients with incident DM (n=19), and manifest DM (n=80). Higher score is indicative of a greater degree of differential expression and thus a higher classification potential. **B,** Classification accuracy. Best classification accuracy was achieved using the top 5 differentially expressed miRNAs. **C,** PCA, a technique that reduces the data to two or more uncorrelated principal components (PC) that explain most of the variance, was used to determine whether control subjects could be distinguished from cohorts with incident and manifest DM. PCA decomposition of the top 5 miRNAs was sufficient to cluster together 91/99 (92%) controls and 56/80 (70%) patients with manifest DM. Interestingly, 10/19 (52%) patients with incident DM were clustered with cases of manifest disease.

subclinical and manifest peripheral artery disease. In detail, miR-126 was associated with a low ankle-brachial index (< 0.9, n=77) (unadjusted and age-/sex-adjusted odds ratio [95% CI] for a 1-SD unit decrease of $\log_e$-transformed expression level of miR-126, 1.95 [1.48 to 2.57], $P<0.001$; and 1.39 [1.04 to 1.86], $P=0.025$) and with new-onset symptomatic peripheral artery disease (1995 to 2005, n=15) (unadjusted and age-/sex-adjusted hazard ratio [95% CI] for a 1-SD unit decrease of $\log_e$-transformed expression level of miR-126, 2.63 [1.38 to 5.02], $P=0.0032$; and 2.15 [1.06 to 4.38], $P=0.030$). In the latter analysis, 37 subjects with symptomatic peripheral artery disease at baseline were excluded.

Discussion

We provide the first evidence for a plasma miRNA signature in patients with DM and a potential prognostic value in this setting. Our findings warrant further investigations into the role of miRNAs in diabetic vascular and myocardial complications.

Plasma MiRNAs in DM

Using differential expression and concepts of network topology, we identified 13 plasma miRNAs in DM including loss of miR-126. Findings were robust in multivariable analyses of patients with DM and age- and sex-matched controls and confirmed in hyperglycemic Lep^{ob} mice. Of note, deregulation

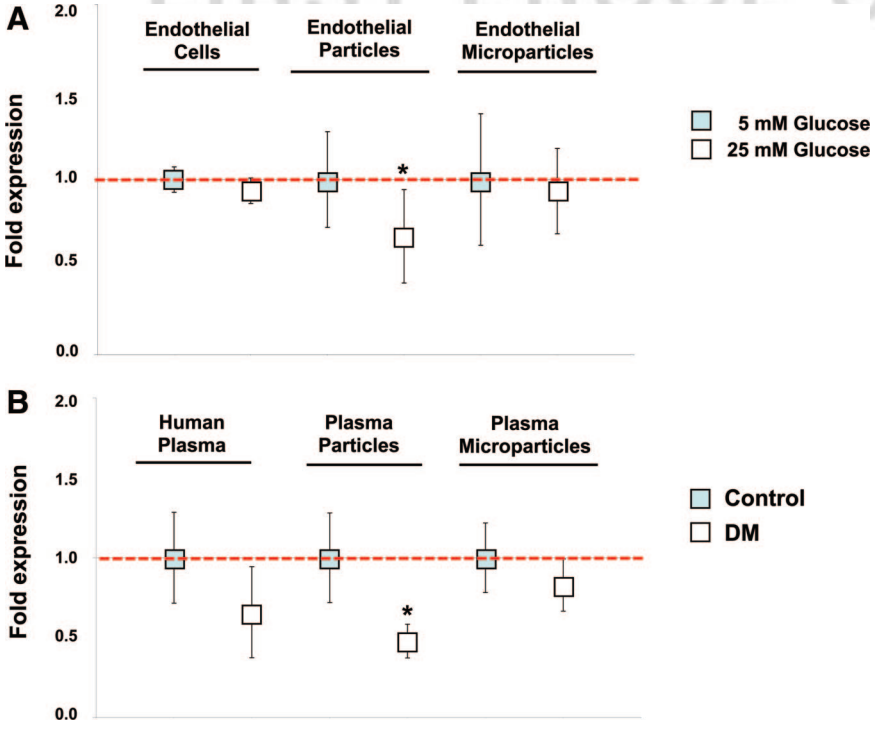

Figure 6. The effect of increased glucose levels on the miR-126 content of vesicles. High glucose concentrations led to a decrease in the miR-126 content of endothelial-derived particles (apoptotic bodies) **(A)** and circulating vesicles in plasma **(B)**. MiRNA expression was assessed using qPCR. miR-454 was used as a normalization control. The data are from 4 independent experiments and presented as means±SEM. *$P<0.05$.

of several plasma miRNAs antedated the manifestation of DM. Principal component analysis (PCA) of the 13 studied miRNAs indicates that 5 miRNAs (miR-15a, miR-126, miR-320, miR-223, miR-28-3p) with the highest scores are necessary and sufficient for a nonredundant classification. Although the function of the highest scoring miRNA, miR-15a is unknown in DM, miR-15a has been previously implicated in cell cycle control and apoptosis in cancer cells.[32] Its expression was shown to inversely correlate with the expression of cyclin D1, although it was also reported to negatively regulate levels of B-cell lymphoma 2 (Bcl-2), a key antiapoptotic protein.[33] In Lep^{ob} mice, however, miR-15a was not significantly different from wild-type mice, probably attributable to low plasma levels. Clinically relevant questions are whether miRNA levels are capable of assessing the probability of DM manifestation in high-risk individuals like patients with impaired fasting glucose, borderline levels of HbA1c or metabolic syndrome, and whether miRNAs can assist in the prediction of micro- and macrovascular complications in DM. Our data suggest that plasma miRNAs might be a useful predictive tool in DM but await confirmation in larger collectives of patients with DM and prediabetes before more definitive comparisons with other standard risk factors can be made. MiR-126, however, deserves special consideration.

MiR-126 and DM

Plasma levels of miR-126 were determined in the entire Bruneck cohort. This is, to our knowledge, the first time a miRNA has been measured in a large population-based study. Whereas most plasma miRNAs are ubiquitously expressed, miR-126 is highly enriched in endothelial cells and plays a pivotal role in maintaining endothelial homeostasis and vascular integrity.[35] It facilitates vascular endothelial growth factor (VEGF) signaling by repressing 2 negative regulators of the VEGF pathway, including the Sprouty-related protein SPRED1 and phosphoinositol-3 kinase regulatory subunit 2 (PIK3R2/p85-β).[34] Plasma miRNAs are packaged in membranous vesicles that change in numbers, cellular origin, and composition depending on the disease state.[36] Accumulating evidence support the notion that these vesicles are not just byproducts resulting from cell activation or apoptosis. Instead, they constitute a novel type of cell–cell mechanism of communication. For example, mir-126 is the most abundant miRNA in endothelial apoptotic bodies.[37] Shedding of miR-126 from endothelial cells has been shown to regulate VEGF responsiveness and to confer vascular protection in a paracrine manner.[37] In our study, loss of miR-126 was consistently associated with DM and the miR-126 content in endothelial apoptotic bodies was reduced in a glucose-dependent fashion. Because apoptotic bodies and microparticles can be transferred to other cell types,[31,37] low plasma levels might result in reduced delivery of miR-126 to monocytes and contribute to VEGF resistance and endothelial dysfunction. This view is corroborated by previous reports that monocytes of patients with DM show impaired responsiveness to VEGF contributing to defects in collateral vessel development[38] and by our finding that loss of miR-126 confers an elevated risk of symptomatic and subclinical peripheral artery disease in the Bruneck population.

Potential Clinical Implications

There are currently no good soluble biomarkers for atherosclerosis and/or endothelial dysfunction. Inflammatory markers such as high-sensitivity C-reactive protein are widely used, but they lack specificity for the vasculature. Moreover, the existing imaging techniques mainly capture the endstage of the disease, eg, the occurrence of plaques, but not its earliest stage such as endothelial dysfunction. If certain plasma miRNAs were uniquely modified by vascular injury, they may be capable of adding to the predictive value of conventional risk factors.

Merits and Limitations

Strengths of our study are its considerable size, representativity for the general community, high methodological standards, control for multiple testing, network analyses, rigorous replication using distinct techniques, various standards (miR-454, RNU6b), and different systems (plasma, cell culture) and species (human, obese mice). As limitations, the particulate fraction in plasma will contain other particles besides endothelial apoptotic bodies and the microarray used for the initial screening did not consider all miRNAs currently known. Accordingly, we cannot claim completeness for the miRNA profile among patients with DM and studies in large collectives of patients with DM and prediabetes are required to assess the potential of the reported miRNA signature and to establish miRNA–drug interactions.

Conclusion

This study provides the first evidence that plasma miRNAs, including endothelial miR-126, are deregulated in patients with DM, which may ultimately lead to novel biomarkers for risk estimation and classification[39] and could be exploited for miRNA-based therapeutic interventions of vascular complications associated with this disease.

Sources of Funding

This work was funded by the British Heart Foundation. M.M. is a Senior Research Fellow of the British Heart Foundation.

Disclosures

None.

References

1. Bartel DP. MicroRNAs: target recognition and regulatory functions. *Cell*. 2009;136:215–233.
2. Pillai RS, Bhattacharyya SN, Filipowicz W. Repression of protein synthesis by miRNAs: how many mechanisms? *Trends Cell Biol*. 2007;17:118–126.
3. Kloosterman WP, Plasterk RH. The diverse functions of microRNAs in animal development and disease. *Dev Cell*. 2006;11:441–450.
4. Latronico MV, Catalucci D, Condorelli G. Emerging role of microRNAs in cardiovascular biology. *Circ Res*. 2007;101:1225–1236.
5. van Rooij E, Marshall WS, Olson EN. Toward microRNA-based therapeutics for heart disease: the sense in antisense. *Circ Res*. 2008;103:919–928.
6. Suarez Y, Fernandez-Hernando C, Pober JS, Sessa WC. Dicer dependent microRNAs regulate gene expression and functions in human endothelial cells. *Circ Res*. 2007;100:1164–1173.
7. Kuehbacher A, Urbich C, Zeiher AM, Dimmeler S. Role of Dicer and Drosha for endothelial microRNA expression and angiogenesis. *Circ Res*. 2007;101:59–68.
8. Mitchell PS, Parkin RK, Kroh EM, Fritz BR, Wyman SK, Pogosova-Agadjanyan EL, Peterson A, Noteboom J, O'Briant KC, Allen A, Lin DW, Urban N, Drescher CW, Knudsen BS, Stirewalt DL, Gentleman R, Vessella RL, Nelson PS, Martin DB, Tewari M. Circulating microRNAs as stable blood-based markers for cancer detection. *Proc Natl Acad Sci U S A*. 2008;105:10513–10518.
9. Tanaka M, Oikawa K, Takanashi M, Kudo M, Ohyashiki J, Ohyashiki K, Kuroda M. Down-regulation of miR-92 in human plasma is a novel marker for acute leukemia patients. *PLoS One*. 2009;4:e5532.

10. Laterza OF, Lim L, Garrett-Engele PW, Vlasakova K, Muniappa N, Tanaka WK, Johnson JM, Sina JF, Fare TL, Sistare FD, Glaab WE. Plasma MicroRNAs as sensitive and specific biomarkers of tissue injury. *Clin Chem*. 2009;55:1977–1983.
11. Wang K, Zhang S, Marzolf B, Troisch P, Brightman A, Hu Z, Hood LE, Galas DJ. Circulating microRNAs, potential biomarkers for drug-induced liver injury. *Proc Natl Acad Sci U S A*. 2009;106:4402–4407.
12. Wang GK, Zhu JQ, Zhang JT, Li Q, Li Y, He J, Qin YW, Jing Q. Circulating microRNA: a novel potential biomarker for early diagnosis of acute myocardial infarction in humans. *Eur Heart J*. 2010;31:659–666.
13. Ji X, Takahashi R, Hiura Y, Hirokawa G, Fukushima Y, Iwai N. Plasma miR-208 as a biomarker of myocardial injury. *Clin Chem*. 2009;55: 1944–1949.
14. Fichtlscherer S, De Rosa S, Fox H, Schwietz T, Fischer A, Liebetrau C, Weber M, Hamm CW, Roxe T, Muller-Ardogan M, Bonauer A, Zeiher AM, Dimmeler S. Circulating microRNAs in patients with coronary artery disease. *Circ Res*. 2010;107.
15. Tijsen AJ, Creemers EE, Moerland PD, de Windt LJ, van der Wal AC, Kok WE, Pinto YM. MiR423–5p as a circulating biomarker for heart failure. *Circ Res*. 2010;106:1035–1039.
16. Nathan DM. Long-term complications of diabetes mellitus. *N Engl J Med*. 1993;328:1676–1685.
17. Frankel DS, Meigs JB, Massaro JM, Wilson PW, O'Donnell CJ, D'Agostino RB, Tofler GH. Von Willebrand factor, type 2 diabetes mellitus, and risk of cardiovascular disease: the framingham offspring study. *Circulation*. 2008;118:2533–2539.
18. Kiechl S, Lorenz E, Reindl M, Wiedermann CJ, Oberhollenzer F, Bonora E, Willeit J, Schwartz DA. Toll-like receptor 4 polymorphisms and atherogenesis. *N Engl J Med*. 2002;347:185–192.
19. Bonora E, Kiechl S, Willeit J, Oberhollenzer F, Egger G, Meigs JB, Bonadonna RC, Muggeo M. Population-based incidence rates and risk factors for type 2 diabetes in white individuals: the Bruneck study. *Diabetes*. 2004;53:1782–1789.
20. Kiechl S, Schett G, Schwaiger J, Seppi K, Eder P, Egger G, Santer P, Mayr A, Xu Q, Willeit J. Soluble receptor activator of nuclear factor-kappa B ligand and risk for cardiovascular disease. *Circulation*. 2007;116:385–391.
21. Hosmer DW, Lemeshow S. *Applied Logistic Regression*. 2nd ed. New York: John Wiley & Sons; 2000.
22. Ramakers C, Ruijter JM, Deprez RH, Moorman AF. Assumption-free analysis of quantitative real-time polymerase chain reaction (PCR) data. *Neurosci Lett*. 2003;339:62–66.
23. Roulston M. Significance testing of information theoretic functionals. *Physica D*. 1997:62–66.
24. Slonim N, Atwal GS, Tkacik G, Bialek W. Information-based clustering. *Proc Natl Acad Sci U S A*. 2005;102:18297–18302.
25. Faith JJ, Hayete B, Thaden JT, Mogno I, Wierzbowski J, Cottarel G, Kasif S, Collins JJ, Gardner TS. Large-scale mapping and validation of Escherichia coli transcriptional regulation from a compendium of expression profiles. *PLoS Biol*. 2007;5:e8.
26. Bansal M, Belcastro V, Ambesi-Impiombato A, di Bernardo D. How to infer gene networks from expression profiles. *Mol Syst Biol*. 2007;3:78.
27. Barabasi AL. Scale-free networks: a decade and beyond. *Science*. 2009; 325:412–413.
28. Chuang HY, Lee E, Liu YT, Lee D, Ideker T. Network-based classification of breast cancer metastasis. *Mol Syst Biol*. 2007;3:140.
29. Tunica DG, Yin X, Sidibe A, Stegemann C, Nissum M, Zeng L, Brunet M, Mayr M. Proteomic analysis of the secretome of human umbilical vein endothelial cells using a combination of free-flow electrophoresis and nanoflow LC-MS/MS. *Proteomics*. 2009;9:4991–4996.
30. Pula G, Mayr U, Evans C, Prokopi M, Vara DS, Yin X, Astroulakis Z, Xiao Q, Hill J, Xu Q, Mayr M. Proteomics identifies thymidine phosphorylase as a key regulator of the angiogenic potential of colony-forming units and endothelial progenitor cell cultures. *Circ Res*. 2009;104:32–40.
31. Prokopi M, Pula G, Mayr U, Devue C, Gallagher J, Xiao Q, Boulanger CM, Westwood N, Urbich C, Willeit J, Steiner M, Breuss J, Xu Q, Kiechl S, Mayr M. Proteomic analysis reveals presence of platelet microparticles in endothelial progenitor cell cultures. *Blood*. 2009;114:723–732.
32. Bandi N, Zbinden S, Gugger M, Arnold M, Kocher V, Hasan L, Kappeler A, Brunner T, Vassella E. miR-15a and miR-16 are implicated in cell cycle regulation in a Rb-dependent manner and are frequently deleted or down-regulated in non-small cell lung cancer. *Cancer Res*. 2009;69:5553–5559.
33. Cimmino A, Calin GA, Fabbri M, Iorio MV, Ferracin M, Shimizu M, Wojcik SE, Aqeilan RI, Zupo S, Dono M, Rassenti L, Alder H, Volinia S, Liu CG, Kipps TJ, Negrini M, Croce CM. miR-15 and miR-16 induce apoptosis by targeting BCL2. *Proc Natl Acad Sci U S A*. 2005;102:13944–13949.
34. Fish JE, Santoro MM, Morton SU, Yu S, Yeh RF, Wythe JD, Ivey KN, Bruneau BG, Stainier DY, Srivastava D. miR-126 regulates angiogenic signaling and vascular integrity. *Dev Cell*. 2008;15:272–284.
35. Wang S, Aurora AB, Johnson BA, Qi X, McAnally J, Hill JA, Richardson JA, Bassel-Duby R, Olson EN. The endothelial-specific microRNA miR-126 governs vascular integrity and angiogenesis. *Dev Cell*. 2008;15:261–271.
36. VanWijk MJ, VanBavel E, Sturk A, Nieuwland R. Microparticles in cardiovascular diseases. *Cardiovasc Res*. 2003;59:277–287.
37. Zernecke A, Bidzhekov K, Noels H, Shagdarsuren E, Gan L, Denecke B, Hristov M, Köppel T, Jahantigh MN, Lutgens E, Wang S, Olson EN, Schober A, Weber C. Delivery of microRNA-126 by apoptotic bodies induces CXCL12-dependent vascular protection. *Sci Signal*. 2009;2:ra81.
38. Waltenberger J, Lange J, Kranz A. Vascular endothelial growth factor-A-induced chemotaxis of monocytes is attenuated in patients with diabetes mellitus: a potential predictor for the individual capacity to develop collaterals. *Circulation*. 2000;102:185–190.
39. Mayr M, Zhang J, Greene AS, Gutterman D, Perloff J, Ping P. Proteomics-based development of biomarkers in cardiovascular disease: mechanistic, clinical, and therapeutic insights. *Mol Cell Proteomics*. 2006;5:1853–1864.

Novelty and Significance

What Is Known?

- MicroRNAs are small noncoding regulatory RNAs that alter protein expression.
- Some microRNAs circulate in plasma vesicles and have been proposed as potential biomarkers for cancer, sepsis, myocardial infarction and heart failure.

What New Information Does This Article Contribute?

- First evidence that plasma miRNAs are deregulated in patients with type 2 diabetes.
- The distinct plasma miRNA pattern in diabetes includes loss of miR-126, a miRNA that is highly enriched in endothelial cells and facilitates VEGF signaling.
- In a population-based study, miR-126 plasma levels negatively correlate with subclinical and manifest peripheral artery disease.

Our study is the first to reveal a plasma miRNA signature in a large population-based cohort of type 2 diabetics. We identified a set of circulating miRNAs that display altered expression in diabetes and characterized dynamic changes in miRNA coexpression networks. This may ultimately lead to novel biomarkers for risk estimation and classification and could be exploited for miRNA-based therapeutic interventions of vascular complications associated with this disease.

Supplemental Material

Plasma miRNA Profiling Reveals Loss of Endothelial MiR-126 and Other MiRNAs in Type II Diabetes

Abbreviations

ABI: ankle-brachial index

CLR: Context likelihood of relatedness

DM: type II diabetes

GLM: General linear models

HUVEC: Human umbilical vein endothelial cells

Lep^{ob}: Leptin obese

MCL: Markov clustering

MiRNA: microRNA

MP: Microparticles

PCA: Principal component analysis

PCC: Pearson correlation coefficient

SVM: Support vector machines

Methods

Clinical history and examination. Smoking status was assessed in each subject [1-5]. Regular alcohol consumption was quantified in terms of grams per day. Hypertension was defined as blood pressure (mean of 3 measurements) ≥ 140/90 mm Hg or the use of antihypertensive drugs. Body mass index was calculated as weight divided by height squared (kg/m^2). Waist and hip circumferences (to the nearest 0.5 cm) were measured by a plastic tape meter at the level of the umbilicus and of the greater trochanters, respectively, and waist-to-hip ratios (WHR) were calculated. Socioeconomic status was assessed on a three-category scale (low, medium, high) based on information about occupational status and educational level of the person with the highest income in the household. Family history of DM refers to first-degree relatives. Physical activity was quantified by the Baecke Score (index for sports activity) [6].

Laboratory methods. Blood samples were drawn after an overnight fast and 12 hours' abstinence from smoking [2-5]. Plasma samples were aliquoted, stored at -80°C and thawed once before analysis. A 75 g oral glucose load (oral glucose tolerance test, OGTT) was administered to all subjects without known DM and blood samples were collected after 120 minutes in order to establish glucose tolerance. High-density lipoprotein (HDL) cholesterol was determined enzymatically (CHOD-PAP method, Merck; CV 2.2% to 2.4%). Low-density lipoprotein (LDL) cholesterol was calculated with the Friedewald formula except in subjects with triglycerides >4.52 mmol/L in whom it was directly measured. Markers of inflammation and all other laboratory parameters were assessed by standard methods as detailed previously [1-5].

Obese mice. All animal experiments were performed according to protocols approved by the Institutional Committee for Use and Care of Laboratory Animals. To determine whether miRNA profiles identified in diabetic subjects also apply to hyperglycaemic animals[7], we quantified plasma levels in obese mice. For this purpose 8-12 week old female Lep^{ob} mice (previously known as ob/ob) (n=6) were purchased from Jackson laboratories. C57BL/6J mice were used as a control (n=6). A total of 1 ml of blood was harvested from each mouse and plasma was isolated following centrifugation at 1,200g for 20 min at 4°C. Plasma samples were aliquoted and stored at -80°C.

RNA isolation from plasma. Total RNA was prepared using the miRNeasy kit (Qiagen) according to the manufacturer's recommendations. In brief, 200 µl of plasma was transferred to an Eppendorf tube and mixed thoroughly with 700µl of QIAzol reagent. Following a brief incubation at ambient temperature, 140 µl of chloroform were added and the solution was mixed vigorously. The samples

were then centrifuged at 12,000 rpm for 15 min at 4°C. The upper aqueous phase was carefully transferred to a new tube and 1.5 volumes of ethanol were added. The samples were then applied directly to columns and washed according to the company's protocol. Total RNA was eluted in 25 µl of nuclease free H_2O. A fixed volume of 3 µl of RNA solution from the 25 µl eluate was used as input in each reverse transcription reaction.

RNA isolation from circulating vesicles. To isolate circulating vesicles, plasma samples from diabetic or healthy subjects were pooled together (30 samples per pool) and three pools were generated per group. Vesicles were isolated by ultracentrifugation. In brief, plasma samples were centrifuged for 10 min at 800g to remove any precipitate and the particulate fraction including apoptotic bodies was then isolated by centrifugation of the supernatant at 10,600 rpm for 20 min. The pellet was resuspended in PBS. An additional centrifugation of the supernatant at 20,500 rpm for 2h was performed to isolate microparticles. The pelleted microparticles were resuspended in PBS and the remaining supernatant was considered as microvesicle-depleted plasma. Total RNA was isolated using the miRNeasy kit as described above.

Reverse transcription and pre-amplification. To assess levels of specific miRNAs in individual plasma samples a fixed volume of 3 µl of RNA solution from the 25 µl eluate was used as input in each reverse transcription (RT) reaction. An RT reaction and pre-amplification step were set up according to the company's recommendations and performed as described above. RT-PCR and pre-amplification products were stored at -20°C. miRNAs were reverse transcribed using the Megaplex Primer Pools (Human Pools A v2.1 and B v2.0) from Applied Biosystems. Pool A enables quantitation of 377 human miRNAs while an additional 290 miRNAs were assessed using Pool B. In each array, three endogenous controls and a negative control were included for data normalization. RT reaction was performed according to the company's recommendations (0.8 µl of Pooled Primers were combined with 0.2 µl of 100mmol/L dNTPs with dTTP, 0.8 µl of 10x Reverse-Transcription Buffer, 0.9 µl of $MgCl_2$ (25mmol/L), 1.5 µl of Multiscribe Reverse-Transcriptase and 0.1 µl of RNAsin (20U/µl) to a final volume of 7.5 µl. The RT-PCR reaction was set as follows: 16°C for 2 min, 42°C for 1 min and 50°C for 1 sec for 40 cycles and then incubation at 85°C for 5 min using a Veriti thermocycler (Applied Biosystems). The RT reaction products were further amplified using the Megaplex PreAmp Primers (Primers A v2.1 and B v2.0). A 2.5 µl aliquot of the RT product was combined with 12.5 µl of Pre-amplification Mastermix (2x) and 2.5 µl of Megaplex PreAmp Primers (10x) to a final volume of 25 µl. The pre-amplification reaction was performed by heating the samples at 95°C for 10 min, followed by 12 cycles of 95°C for 15 sec and 60°C for 4 min. Finally, samples were heated at 95°C for 10 min to ensure enzyme inactivation. Pre-amplification reaction products were diluted to a final volume of 100 µl and stored at -20°C.

Taqman miRNA array. The expression profile of miRNAs in plasma samples was determined using the Human Taqman miRNA Arrays A and B (Applied Biosystems). PCR reactions were performed using 450 µl of the Taqman Universal PCR Master Mix No AmpErase UNG (2x) and 9 µl of the diluted pre-amplification product to a final volume of 900 µl. 100µl of the PCR mix was dispensed to each port of the Taqman miRNA Array. The fluidic card was then centrifuged and mechanically sealed. QPCR was carried out on an Applied Biosystems 7900HT thermocycler using the manufacturer's recommended programme. Detailed analysis of the results was performed using the Real-Time Statminer Software (Integromics).

Taqman qPCR assay. Taqman miRNA assays were used to assess the expression of individual miRNAs. 0.5µl of the diluted pre-amplification product were combined with 0.25 µl of Taqman miRNA Assay (20x) (Applied Biosystems) and 2.5 µl of the Taqman Universal PCR Master Mix No AmpErase UNG (2x) to a final volume of 5 µl. QPCR was performed on an Applied Biosystems 7900HT thermocycler at 95°C for 10 min, followed by 40 cycles of 95°C for 15 sec and 60°C for 1 min. All samples were run in duplicates and standardized to miR-454 and RNU6b using SDS2.2 (Applied Biosystems) software. For sensitivity analyses, levels of miRNAs for PCR efficacy were corrected using the LinRegPCR software.

Network clustering. Modular structure of the miRNA co-expression network was identified using the Markov Clustering (MCL) algorithm [8]. This is an efficient, unsupervised, and highly accurate graph clustering approach based on graph flow simulation [9]. A distinct advantage of MCL is its ability to avoid incorrect clustering assignments in the presence of false negative edges. This is due to the fact that MCL discovers clusters by virtue of miRNAs sharing higher-order connectivity in their local neighborhood and not merely pair-wise linkages.

MiRNA feature selection, principal component analysis (PCA), and classification. Of the 30 differentially expressed miRNAs, 13 targets with extreme distributions in node degree, clustering coefficient, and eigenvector centrality were selected for qPCR validation. Predictive significance of validated miRNAs was calculated using bootstrap aggregation for an ensemble of 10,000 decision trees. Each miRNA profile was assigned an importance value based on how well it can differentiate control, incident DM, and manifest DM cases. The discriminatory power of the PCA was quantified using the Support Vector Machines (SVM) algorithm, a supervised learning method. SVM were trained on half of the data selected at random and validated on the remaining samples. This procedure was repeated 10 times and the final correct classification rate was presented as an average of all SVM iterations.

Ascertainment of peripheral artery disease. The ankle-brachial index (ABI) was measured in a supine position. A cuff was inflated to 10 mmHg above systolic blood pressure and deflated at 2 mmHg/s. The first reappearance of the arterial signal at the ankle (posterior tibial artery) was taken as the systolic blood pressure (detected with a Doppler ultrasonic instrument). To calculate the ABI for the right and left leg, the systolic blood pressure at each ankle was divided by the systolic blood pressure in the arm. The higher arm reading (right or left side) was used for ABI calculation. An ABI < 0.9 was considered indicative of peripheral artery disease (low ABI). The diagnosis of new-onset (1995-2005) symptomatic peripheral artery disease required (1) a positive response to the Rose questionnaire (intermittent claudication) with the vascular nature of complaints confirmed by standard diagnostic procedures (ankle-brachial pressure index, ultrasound or angiography) or (2) an acute peripheral artery occlusion necessitating revascularization (angioplasty and surgery). Ascertainment of events did not rely on hospital discharge codes or the patient's self-report but on a careful review of medical records provided by the general practitioners, death certificates, and Bruneck Hospital files, and the extensive clinical and laboratory examinations performed as part of the study protocols. Major advantages of the Bruneck Study are that virtually all subjects living in the Bruneck area were referred to the local hospital and that the network existing between the local hospital and the general practitioners allowed retrieval of practically all medical information on persons living in the area.

References

1. Bonora E, Kiechl S, Willeit J, Oberhollenzer F, Egger G, Meigs JB, Bonadonna RC, Muggeo M. Population-based incidence rates and risk factors for type 2 diabetes in white individuals: the Bruneck study. *Diabetes.* 2004;53:1782-1789.
2. Tsimikas S, Willeit J, Knoflach M, Mayr M, Egger G, Notdurfter M, Witztum JL, Wiedermann CJ, Xu Q, Kiechl S. Lipoprotein-associated phospholipase A2 activity, ferritin levels, metabolic syndrome, and 10-year cardiovascular and non-cardiovascular mortality: results from the Bruneck study. *Eur Heart J.* 2009;30:107-115.
3. Kiechl S, Lorenz E, Reindl M, Wiedermann CJ, Oberhollenzer F, Bonora E, Willeit J, Schwartz DA. Toll-like receptor 4 polymorphisms and atherogenesis. *N Engl J Med.* 2002;347:185-192.
4. Kiechl S, Schett G, Schwaiger J, Seppi K, Eder P, Egger G, Santer P, Mayr A, Xu Q, Willeit J. Soluble receptor activator of nuclear factor-kappa B ligand and risk for cardiovascular disease. *Circulation.* 2007;116:385-391.
5. Kiechl S, Willeit J, Mayr M, Viehweider B, Oberhollenzer M, Kronenberg F, Wiedermann CJ, Oberthaler S, Xu Q, Witztum JL, Tsimikas S. Oxidized phospholipids, lipoprotein(a), lipoprotein-associated phospholipase A2 activity, and 10-year cardiovascular outcomes: prospective results from the Bruneck study. *Arterioscler Thromb Vasc Biol.* 2007;27:1788-1795.
6. Baecke JA, Burema J, Frijters JE. A short questionnaire for the measurement of habitual physical activity in epidemiological studies. *Am J Clin Nutr.* 1982;36:936-942.
7. Coleman DL. Obese and diabetes: two mutant genes causing diabetes-obesity syndromes in mice. *Diabetologia.* 1978;14:141-148.
8. van Dongen S. *Graph clustering by flow simulation* [PhD], University of Utrecht; 2000.
9. Enright AJ, Van Dongen S, Ouzounis CA. An efficient algorithm for large-scale detection of protein families. *Nucleic Acids Res.* 2002;30:1575-1584.

Online Table I. Characteristics of patients with manifest DM and age-/sex-matched controls (Bruneck Study).

Characteristic*	DM (n=80)	Control (n=80)
Demographic variables		
Age, years	66.3±8.9	66.3±8.9
Female sex, n (%)	50 (62.5)	50 (62.5)
Social status, n (%)		
Low	60 (75.0)	51 (63.8)
Middle	10 (12.5)	15 (18.8)
High	10 (12.5)	14 (17.5)
Lifestyle and diabetes risk factors		
Smoking, n (%)	9 (11.3)	10 (12.5)
Family history of diabetes, n (%)	26 (32.5)	17 (21.3)
Alcohol consumption, grams/day	18.6±28.9	18.4±25.0
Physical activity (sport index)	1.7±0.9	2.2±0.8
Body mass index, kg/m²	28.0±4.4	25.0±4.0
Waist-to-hip ratio, cm/cm	0.95±0.07	0.92±0.08
Hypertension, n (%)	71 (88.8)	58 (72.5)
HDL cholesterol, mg/dL	53.9±13.7	62.7±19.5
LDL cholesterol, mg/dL	146.2±39.1	140.4±35.2
Triglycerides, mg/dL	141[99-186]	91[73-125]
High-sensitivity CRP, mg/L	3.0[1.6-6.5]	1.9[0.9-3.0]
Glycaemia		
Fasting glucose, mg/dL	139.0±50.0	91.6±5.9
2-hr glucose, mg/dL	232.6±81.6	94.1±21.5
Glycated hemoglobin (Hba1c), %	6.5±1.4	5.4±0.3

* Values presented are unadjusted means ± SD, medians [IQR] or numbers (percentages).

Online Table II. Circulating miRNAs and differentially expressed miRNAs in DM.

Identified Targets	Ct values (cycles)
miR-17, miR-92a, miR-106a, miR-146a, **miR-150**, **miR-191**, **miR-223**, **miR-320**, miR-484	22-25
miR-16, miR-19b, miR-20a, **miR-20b**, **miR-24**, **miR-28-3p**, **miR-29b**, miR-30b, miR-30c, miR-106b, **miR-126**, **miR-197**, miR-222, miR-331, **miR-342-3p**, miR-483-5p	25-28
let-7e, miR-10a, **miR-21**, miR-29a, miR-93, miR-106b, miR-133, **miR-139-5p**, miR-145, **miR-146b-5p**, miR-185, miR-186, miR-199a, miR-328, miR-425, miR-486-3p, miR-495, **miR-574-3p**	28-30
let-7f, **let-7b**, **miR-15a**, miR-19a, **miR-25**, miR-26a, miR-27a, miR-28-5p, **miR-99b**, miR-100, miR-103, **miR-122**, **miR-125-5p**, miR-127-3p, **miR-134**, **miR-139-3p**, **miR-140-5p**, miR-142-3p, miR-152, miR-193-5p, miR-204, miR-221, miR-224, miR-339-3p, miR-345, miR-375, miR-376a, **miR-423-5p**, **miR-433**, miR-454, **miR-486-5p**, miR-491-5p, miR-517a, miR-532-3p, miR-539, miR-744, **miR-885-5p**, miR-886-3p,	30-32
let-7c, let-7f, let-7g, miR-1, miR-9, miR-10b, miR-15b, miR-23a, miR-28-5p, miR-32, miR-101, miR-129-3p, miR-138, miR-140, miR-143,miR-148a, miR-181a, miR-192, miR-193a-3p, miR-193b, miR-195, miR-198, miR-204, miR-301a, miR-324, miR-330-3p, miR-331, miR-335, miR-361-5p, miR-365, miR-374a, miR-374b, miR-411, miR-451, miR-486-3p, miR- 494, miR-502-3p, miR-519e, miR-520d-5p, miR-532-3p, miR-532-5p, miR-548a-3p, miR-590-5p, miR-598, miR-625, miR-629, miR-636, miR-652, miR-660, miR-886-5p, miR-376c, miR-30e*, miR-505*, miR-130b*, miR-93*, miR-99b*, miR-541*, miR-425*, miR-19b-1*, miR-643, miR-610, miR-520c, miR-513-3p, miR-509-3p, miR-30a, miR-572, miR-571	32-35

Bold font highlights differentially expressed miRNAs in DM

Online Table III. miRNA-miRNA co-expression network

Node A	Node B	PCC
let-7b	let-7d	0.86
let-7c	miR-100	0.86
let-7d	miR-106b	0.86
miR-103	miR-106b	0.99
miR-106a	miR-106b	0.85
let-7d	miR-122	0.87
miR-106a	miR-126	0.97
miR-103	miR-127-3p	0.90
miR-106a	miR-127-3p	0.91
miR-106b	miR-127-3p	0.90
miR-126	miR-127-3p	0.85
miR-1	miR-129-3p	0.91
let-7e	miR-133a	0.90
miR-103	miR-133a	0.85
miR-106a	miR-133a	0.87
miR-106b	miR-133a	0.87
miR-126	miR-133a	0.88
miR-127-3p	miR-133a	0.89
miR-101	miR-138	0.91
miR-103	miR-139-3p	0.86
miR-106a	miR-139-3p	0.90
miR-127-3p	miR-139-3p	0.95
let-7d	miR-139-5p	0.86
miR-106a	miR-139-5p	0.94
miR-122	miR-139-5p	0.88
miR-126	miR-139-5p	0.92
miR-127-3p	miR-139-5p	0.87
miR-103	miR-140-3p	0.88
miR-139-3p	miR-140-3p	0.89
let-7e	miR-140-5p	0.88
miR-106a	miR-140-5p	0.88
miR-126	miR-140-5p	0.87
miR-127-3p	miR-140-5p	0.88
miR-133a	miR-140-5p	0.93
miR-139-3p	miR-140-5p	0.88
let-7e	miR-142-3p	0.88
let-7e	miR-145	0.86
miR-103	miR-145	0.90
miR-106a	miR-145	0.89
miR-106b	miR-145	0.89
miR-126	miR-145	0.89
miR-127-3p	miR-145	0.92
miR-133a	miR-145	0.96
miR-139-3p	miR-145	0.91
miR-140-5p	miR-145	0.96
miR-142-3p	miR-145	0.85
miR-106a	miR-146a	0.91
miR-126	miR-146a	0.94
miR-140-5p	miR-146a	0.85

miR-143	miR-146a	0.88
miR-103	miR-148a	0.88
miR-140-3p	miR-148a	0.86
miR-126	miR-150	0.91
miR-146a	miR-150	0.93
miR-146b-5p	miR-150	0.96
let-7c	miR-15a	0.89
miR-103	miR-15b	0.94
miR-106a	miR-15b	0.88
miR-106b	miR-15b	0.92
miR-126	miR-15b	0.86
miR-139-3p	miR-15b	0.86
miR-145	miR-15b	0.89
miR-146a	miR-15b	0.86
miR-106a	miR-16	0.87
miR-126	miR-16	0.89
miR-146a	miR-16	0.93
miR-15b	miR-16	0.93
let-7e	miR-17	0.90
miR-103	miR-17	0.88
miR-106a	miR-17	0.92
miR-106b	miR-17	0.88
miR-126	miR-17	0.93
miR-127-3p	miR-17	0.87
miR-133a	miR-17	0.94
miR-139-3p	miR-17	0.86
miR-140-5p	miR-17	0.95
miR-142-3p	miR-17	0.87
miR-145	miR-17	0.98
miR-146a	miR-17	0.91
miR-15b	miR-17	0.92
miR-16	miR-17	0.87
let-7e	miR-181a	0.90
miR-133a	miR-181a	0.87
miR-140-5p	miR-181a	0.97
miR-145	miR-181a	0.91
miR-17	miR-181a	0.90
let-7e	miR-185	0.89
miR-133a	miR-185	0.86
miR-142-3p	miR-185	0.98
miR-145	miR-185	0.87
miR-17	miR-185	0.90
miR-126	miR-186	0.89
miR-133a	miR-186	0.85
miR-140-5p	miR-186	0.88
miR-142-3p	miR-186	0.86
miR-145	miR-186	0.94
miR-146a	miR-186	0.92
miR-15b	miR-186	0.92
miR-16	miR-186	0.93
miR-17	miR-186	0.96
miR-181a	miR-186	0.85

miR-185	miR-186	0.88
miR-143	miR-191	0.89
let-7d	miR-192	0.85
miR-103	miR-192	0.98
miR-106a	miR-192	0.90
miR-106b	miR-192	0.99
miR-126	miR-192	0.87
miR-127-3p	miR-192	0.91
miR-133a	miR-192	0.89
miR-139-3p	miR-192	0.86
miR-139-5p	miR-192	0.88
miR-145	miR-192	0.92
miR-15b	miR-192	0.96
miR-17	miR-192	0.93
miR-186	miR-192	0.87
miR-103	miR-193a-5p	0.94
miR-106b	miR-193a-5p	0.93
miR-133a	miR-193a-5p	0.86
miR-142-3p	miR-193a-5p	0.90
miR-145	miR-193a-5p	0.92
miR-15b	miR-193a-5p	0.94
miR-17	miR-193a-5p	0.94
miR-185	miR-193a-5p	0.94
miR-186	miR-193a-5p	0.91
miR-192	miR-193a-5p	0.95
let-7d	miR-193b	0.86
miR-103	miR-193b	0.91
miR-106a	miR-193b	0.96
miR-106b	miR-193b	0.94
miR-126	miR-193b	0.94
miR-127-3p	miR-193b	0.94
miR-133a	miR-193b	0.88
miR-139-3p	miR-193b	0.87
miR-139-5p	miR-193b	0.95
miR-140-5p	miR-193b	0.87
miR-145	miR-193b	0.92
miR-15b	miR-193b	0.91
miR-16	miR-193b	0.88
miR-17	miR-193b	0.94
miR-186	miR-193b	0.86
miR-192	miR-193b	0.96
miR-193a-5p	miR-193b	0.88
miR-181a	miR-195	0.88
let-7e	miR-197	0.85
miR-103	miR-197	0.90
miR-106a	miR-197	0.93
miR-106b	miR-197	0.91
miR-126	miR-197	0.95
miR-127-3p	miR-197	0.87
miR-133a	miR-197	0.92
miR-139-3p	miR-197	0.86
miR-139-5p	miR-197	0.86

miR-140-5p	miR-197	0.90
miR-145	miR-197	0.96
miR-146a	miR-197	0.91
miR-15b	miR-197	0.96
miR-16	miR-197	0.91
miR-17	miR-197	0.98
miR-185	miR-197	0.89
miR-186	miR-197	0.96
miR-192	miR-197	0.95
miR-193a-5p	miR-197	0.94
miR-193b	miR-197	0.94
miR-138	miR-198	0.89
miR-133a	miR-199a-3p	0.86
miR-140-3p	miR-199a-3p	0.85
miR-140-5p	miR-199a-3p	0.93
miR-145	miR-199a-3p	0.86
miR-181a	miR-199a-3p	0.91
miR-133a	miR-19a	0.87
miR-140-5p	miR-19a	0.87
miR-142-3p	miR-19a	0.92
miR-145	miR-19a	0.94
miR-146a	miR-19a	0.87
miR-15b	miR-19a	0.90
miR-16	miR-19a	0.87
miR-17	miR-19a	0.95
miR-181a	miR-19a	0.85
miR-185	miR-19a	0.93
miR-186	miR-19a	0.99
miR-192	miR-19a	0.86
miR-193a-5p	miR-19a	0.92
miR-197	miR-19a	0.95
let-7d	miR-19b	0.86
miR-103	miR-19b	0.88
miR-106a	miR-19b	0.94
miR-106b	miR-19b	0.91
miR-126	miR-19b	0.96
miR-127-3p	miR-19b	0.87
miR-133a	miR-19b	0.89
miR-139-5p	miR-19b	0.92
miR-145	miR-19b	0.92
miR-146a	miR-19b	0.89
miR-15b	miR-19b	0.95
miR-16	miR-19b	0.91
miR-17	miR-19b	0.95
miR-186	miR-19b	0.93
miR-192	miR-19b	0.95
miR-193a-5p	miR-19b	0.90
miR-193b	miR-19b	0.95
miR-197	miR-19b	0.99
miR-19a	miR-19b	0.91
let-7d	miR-204	0.87
miR-103	miR-204	0.88

miR-106a	miR-204	0.93
miR-106b	miR-204	0.91
miR-122	miR-204	0.86
miR-126	miR-204	0.95
miR-127-3p	miR-204	0.87
miR-133a	miR-204	0.87
miR-139-5p	miR-204	0.93
miR-145	miR-204	0.90
miR-146a	miR-204	0.88
miR-15b	miR-204	0.95
miR-16	miR-204	0.92
miR-17	miR-204	0.93
miR-186	miR-204	0.91
miR-192	miR-204	0.96
miR-193a-5p	miR-204	0.89
miR-193b	miR-204	0.95
miR-197	miR-204	0.98
miR-19a	miR-204	0.89
miR-19b	miR-204	1.00
let-7d	miR-20a	0.89
miR-103	miR-20a	0.90
miR-106b	miR-20a	0.94
miR-122	miR-20a	0.88
miR-127-3p	miR-20a	0.90
miR-133a	miR-20a	0.88
miR-139-5p	miR-20a	0.89
miR-145	miR-20a	0.85
miR-15b	miR-20a	0.85
miR-192	miR-20a	0.94
miR-193b	miR-20a	0.91
miR-197	miR-20a	0.88
miR-19b	miR-20a	0.92
miR-204	miR-20a	0.92
miR-106a	miR-20b	0.92
miR-106b	miR-20b	0.87
miR-122	miR-20b	0.87
miR-126	miR-20b	0.88
miR-127-3p	miR-20b	0.88
miR-139-5p	miR-20b	0.94
miR-192	miR-20b	0.89
miR-193b	miR-20b	0.90
miR-19b	miR-20b	0.90
miR-204	miR-20b	0.90
miR-20a	miR-20b	0.93
miR-103	miR-21	0.89
miR-106a	miR-21	0.95
miR-106b	miR-21	0.91
miR-126	miR-21	0.92
miR-127-3p	miR-21	0.98
miR-133a	miR-21	0.93
miR-139-3p	miR-21	0.92
miR-139-5p	miR-21	0.92

miR-140-5p	miR-21	0.87
miR-145	miR-21	0.93
miR-15b	miR-21	0.87
miR-17	miR-21	0.90
miR-192	miR-21	0.93
miR-193b	miR-21	0.96
miR-197	miR-21	0.92
miR-19b	miR-21	0.93
miR-204	miR-21	0.93
miR-20a	miR-21	0.94
miR-20b	miR-21	0.94
miR-103	miR-221	0.93
miR-106b	miR-221	0.92
miR-148a	miR-221	0.94
miR-192	miR-221	0.87
miR-193a-5p	miR-221	0.86
let-7e	miR-222	0.87
miR-106a	miR-222	0.91
miR-126	miR-222	0.93
miR-140-5p	miR-222	0.94
miR-145	miR-222	0.87
miR-146a	miR-222	0.93
miR-150	miR-222	0.89
miR-17	miR-222	0.91
miR-181a	miR-222	0.92
miR-186	miR-222	0.85
miR-191	miR-222	0.85
miR-197	miR-222	0.87
let-7e	miR-223	0.90
miR-103	miR-223	0.86
miR-106a	miR-223	0.95
miR-106b	miR-223	0.88
miR-126	miR-223	0.96
miR-127-3p	miR-223	0.92
miR-133a	miR-223	0.95
miR-139-3p	miR-223	0.87
miR-139-5p	miR-223	0.88
miR-140-5p	miR-223	0.95
miR-145	miR-223	0.97
miR-146a	miR-223	0.88
miR-15b	miR-223	0.88
miR-16	miR-223	0.86
miR-17	miR-223	0.98
miR-181a	miR-223	0.90
miR-186	miR-223	0.92
miR-192	miR-223	0.92
miR-193a-5p	miR-223	0.88
miR-193b	miR-223	0.97
miR-197	miR-223	0.97
miR-19a	miR-223	0.91
miR-19b	miR-223	0.95
miR-204	miR-223	0.94

miR-20a	miR-223	0.87
miR-21	miR-223	0.95
miR-222	miR-223	0.92
miR-103	miR-24	0.88
miR-106a	miR-24	0.97
miR-106b	miR-24	0.90
miR-126	miR-24	0.97
miR-127-3p	miR-24	0.92
miR-133a	miR-24	0.91
miR-139-3p	miR-24	0.89
miR-139-5p	miR-24	0.92
miR-140-5p	miR-24	0.91
miR-145	miR-24	0.95
miR-146a	miR-24	0.92
miR-15b	miR-24	0.93
miR-16	miR-24	0.92
miR-17	miR-24	0.97
miR-186	miR-24	0.93
miR-192	miR-24	0.94
miR-193a-5p	miR-24	0.89
miR-193b	miR-24	0.98
miR-197	miR-24	0.98
miR-19a	miR-24	0.90
miR-19b	miR-24	0.98
miR-204	miR-24	0.97
miR-20a	miR-24	0.88
miR-20b	miR-24	0.88
miR-21	miR-24	0.95
miR-222	miR-24	0.90
miR-223	miR-24	0.99
miR-106a	miR-25	0.96
miR-126	miR-25	0.91
miR-127-3p	miR-25	0.97
miR-139-3p	miR-25	0.94
miR-139-5p	miR-25	0.90
miR-140-5p	miR-25	0.90
miR-145	miR-25	0.90
miR-17	miR-25	0.88
miR-192	miR-25	0.86
miR-193b	miR-25	0.94
miR-197	miR-25	0.87
miR-19b	miR-25	0.86
miR-204	miR-25	0.86
miR-20b	miR-25	0.86
miR-21	miR-25	0.96
miR-222	miR-25	0.87
miR-223	miR-25	0.93
miR-24	miR-25	0.94
miR-122	miR-26a	0.94
miR-125a-5p	miR-26a	0.90
miR-139-5p	miR-26a	0.94
miR-193b	miR-26a	0.85

miR-204	miR-26a	0.86
miR-20a	miR-26a	0.89
miR-20b	miR-26a	0.96
miR-21	miR-26a	0.87
miR-106a	miR-28-3p	0.90
miR-126	miR-28-3p	0.87
miR-127-3p	miR-28-3p	0.91
miR-139-3p	miR-28-3p	0.93
miR-140-5p	miR-28-3p	0.96
miR-145	miR-28-3p	0.92
miR-146a	miR-28-3p	0.87
miR-17	miR-28-3p	0.90
miR-181a	miR-28-3p	0.90
miR-186	miR-28-3p	0.86
miR-193b	miR-28-3p	0.88
miR-195	miR-28-3p	0.90
miR-197	miR-28-3p	0.86
miR-21	miR-28-3p	0.89
miR-222	miR-28-3p	0.92
miR-223	miR-28-3p	0.93
miR-24	miR-28-3p	0.91
miR-25	miR-28-3p	0.96
miR-106a	miR-28-5p	0.90
miR-126	miR-28-5p	0.87
miR-129-3p	miR-28-5p	0.88
miR-146b-5p	miR-28-5p	0.85
miR-150	miR-28-5p	0.85
miR-222	miR-28-5p	0.90
miR-146b-5p	miR-29b	0.97
miR-150	miR-29b	0.94
miR-191	miR-29c	0.92
let-7e	miR-301a	0.86
let-7d	miR-30b	0.86
let-7e	miR-30b	0.93
miR-106a	miR-30b	0.89
miR-106b	miR-30b	0.87
miR-126	miR-30b	0.93
miR-127-3p	miR-30b	0.88
miR-133a	miR-30b	0.95
miR-139-5p	miR-30b	0.85
miR-140-5p	miR-30b	0.92
miR-142-3p	miR-30b	0.89
miR-145	miR-30b	0.95
miR-17	miR-30b	0.97
miR-181a	miR-30b	0.89
miR-185	miR-30b	0.88
miR-186	miR-30b	0.92
miR-192	miR-30b	0.91
miR-193a-5p	miR-30b	0.89
miR-193b	miR-30b	0.94
miR-197	miR-30b	0.95
miR-19a	miR-30b	0.92

miR-19b	miR-30b	0.94
miR-204	miR-30b	0.93
miR-20a	miR-30b	0.89
miR-21	miR-30b	0.92
miR-222	miR-30b	0.87
miR-223	miR-30b	0.98
miR-24	miR-30b	0.96
miR-25	miR-30b	0.86
miR-28-3p	miR-30b	0.86
let-7e	miR-30c	0.86
miR-103	miR-30c	0.86
miR-106a	miR-30c	0.92
miR-106b	miR-30c	0.87
miR-126	miR-30c	0.95
miR-127-3p	miR-30c	0.88
miR-133a	miR-30c	0.95
miR-139-3p	miR-30c	0.86
miR-140-5p	miR-30c	0.91
miR-142-3p	miR-30c	0.85
miR-145	miR-30c	0.97
miR-146a	miR-30c	0.90
miR-15b	miR-30c	0.92
miR-16	miR-30c	0.88
miR-17	miR-30c	0.98
miR-185	miR-30c	0.89
miR-186	miR-30c	0.96
miR-192	miR-30c	0.92
miR-193a-5p	miR-30c	0.90
miR-193b	miR-30c	0.92
miR-197	miR-30c	0.99
miR-19a	miR-30c	0.96
miR-19b	miR-30c	0.97
miR-204	miR-30c	0.96
miR-20a	miR-30c	0.88
miR-21	miR-30c	0.93
miR-222	miR-30c	0.88
miR-223	miR-30c	0.97
miR-24	miR-30c	0.97
miR-25	miR-30c	0.86
miR-28-3p	miR-30c	0.87
miR-30b	miR-30c	0.96
miR-106a	miR-320	0.90
miR-126	miR-320	0.94
miR-140-5p	miR-320	0.89
miR-143	miR-320	0.89
miR-146a	miR-320	0.98
miR-150	miR-320	0.94
miR-16	miR-320	0.87
miR-17	miR-320	0.90
miR-181a	miR-320	0.85
miR-186	miR-320	0.89
miR-191	miR-320	0.86

miR-197	miR-320	0.88
miR-19b	miR-320	0.86
miR-222	miR-320	0.98
miR-223	miR-320	0.89
miR-24	miR-320	0.91
miR-28-3p	miR-320	0.90
miR-28-5p	miR-320	0.87
miR-30c	miR-320	0.88
miR-139-3p	miR-323-3p	0.86
miR-25	miR-323-3p	0.85
miR-103	miR-324-3p	0.95
miR-106a	miR-324-3p	0.91
miR-106b	miR-324-3p	0.96
miR-126	miR-324-3p	0.90
miR-127-3p	miR-324-3p	0.89
miR-133a	miR-324-3p	0.89
miR-139-3p	miR-324-3p	0.88
miR-139-5p	miR-324-3p	0.87
miR-145	miR-324-3p	0.93
miR-15b	miR-324-3p	0.98
miR-16	miR-324-3p	0.88
miR-17	miR-324-3p	0.94
miR-186	miR-324-3p	0.90
miR-192	miR-324-3p	0.99
miR-193a-5p	miR-324-3p	0.94
miR-193b	miR-324-3p	0.94
miR-197	miR-324-3p	0.98
miR-19a	miR-324-3p	0.89
miR-19b	miR-324-3p	0.98
miR-204	miR-324-3p	0.98
miR-20a	miR-324-3p	0.92
miR-20b	miR-324-3p	0.90
miR-21	miR-324-3p	0.93
miR-223	miR-324-3p	0.92
miR-24	miR-324-3p	0.95
miR-25	miR-324-3p	0.85
miR-30b	miR-324-3p	0.90
miR-30c	miR-324-3p	0.95
let-7e	miR-328	0.86
miR-106a	miR-328	0.87
miR-126	miR-328	0.87
miR-127-3p	miR-328	0.91
miR-133a	miR-328	0.94
miR-139-3p	miR-328	0.89
miR-140-5p	miR-328	0.99
miR-145	miR-328	0.98
miR-17	miR-328	0.96
miR-181a	miR-328	0.96
miR-186	miR-328	0.92
miR-192	miR-328	0.86
miR-193a-5p	miR-328	0.86
miR-193b	miR-328	0.90

miR-195	miR-328	0.86
miR-197	miR-328	0.92
miR-199a-3p	miR-328	0.89
miR-19a	miR-328	0.91
miR-19b	miR-328	0.86
miR-21	miR-328	0.90
miR-222	miR-328	0.90
miR-223	miR-328	0.97
miR-24	miR-328	0.93
miR-25	miR-328	0.91
miR-28-3p	miR-328	0.96
miR-30b	miR-328	0.94
miR-30c	miR-328	0.93
miR-320	miR-328	0.86
miR-324-3p	miR-328	0.86
miR-129-3p	miR-330-3p	0.89
miR-146a	miR-330-3p	0.91
miR-222	miR-330-3p	0.87
miR-28-5p	miR-330-3p	0.90
miR-320	miR-330-3p	0.90
let-7e	miR-331-3p	0.92
miR-103	miR-331-3p	0.86
miR-106a	miR-331-3p	0.89
miR-106b	miR-331-3p	0.88
miR-126	miR-331-3p	0.92
miR-133a	miR-331-3p	0.97
miR-140-5p	miR-331-3p	0.91
miR-142-3p	miR-331-3p	0.89
miR-145	miR-331-3p	0.96
miR-146a	miR-331-3p	0.86
miR-15b	miR-331-3p	0.88
miR-17	miR-331-3p	0.98
miR-181a	miR-331-3p	0.86
miR-185	miR-331-3p	0.93
miR-186	miR-331-3p	0.93
miR-192	miR-331-3p	0.92
miR-193a-5p	miR-331-3p	0.93
miR-193b	miR-331-3p	0.90
miR-197	miR-331-3p	0.97
miR-19a	miR-331-3p	0.94
miR-19b	miR-331-3p	0.95
miR-204	miR-331-3p	0.93
miR-20a	miR-331-3p	0.86
miR-21	miR-331-3p	0.89
miR-222	miR-331-3p	0.87
miR-223	miR-331-3p	0.96
miR-24	miR-331-3p	0.95
miR-30b	miR-331-3p	0.96
miR-30c	miR-331-3p	0.98
miR-320	miR-331-3p	0.85
miR-324-3p	miR-331-3p	0.94
miR-328	miR-331-3p	0.92

miR-101	miR-331-5p	0.99
miR-138	miR-331-5p	0.90
miR-198	miR-331-5p	0.87
miR-106a	miR-342-3p	0.93
miR-126	miR-342-3p	0.96
miR-139-5p	miR-342-3p	0.89
miR-146a	miR-342-3p	0.92
miR-146b-5p	miR-342-3p	0.92
miR-150	miR-342-3p	0.97
miR-193b	miR-342-3p	0.86
miR-19b	miR-342-3p	0.87
miR-204	miR-342-3p	0.86
miR-222	miR-342-3p	0.93
miR-223	miR-342-3p	0.88
miR-24	miR-342-3p	0.90
miR-28-5p	miR-342-3p	0.91
miR-29b	miR-342-3p	0.92
miR-320	miR-342-3p	0.94
let-7e	miR-345	0.87
miR-142-3p	miR-345	0.94
miR-17	miR-345	0.89
miR-185	miR-345	0.96
miR-186	miR-345	0.90
miR-193a-5p	miR-345	0.92
miR-197	miR-345	0.86
miR-19a	miR-345	0.93
miR-331-3p	miR-345	0.88
miR-335	miR-361-5p	1.00
miR-301a	miR-365	0.99
miR-103	miR-370	0.92
miR-106b	miR-370	0.87
miR-140-3p	miR-370	0.92
miR-145	miR-370	0.86
miR-148a	miR-370	0.97
miR-15b	miR-370	0.87
miR-192	miR-370	0.87
miR-193a-5p	miR-370	0.88
miR-221	miR-370	0.90
miR-328	miR-370	0.85
let-7d	miR-374a	0.86
miR-122	miR-374a	0.90
miR-20b	miR-374a	0.85
miR-26a	miR-374a	0.88
miR-339-3p	miR-374a	0.85
miR-103	miR-374b	0.91
miR-106b	miR-374b	0.86
miR-140-3p	miR-374b	0.89
miR-148a	miR-374b	0.97
miR-15b	miR-374b	0.86
miR-193a-5p	miR-374b	0.87
miR-221	miR-374b	0.90
miR-370	miR-374b	0.96

let-7d	miR-375	0.88
miR-103	miR-375	0.93
miR-106a	miR-375	0.87
miR-106b	miR-375	0.96
miR-122	miR-375	0.88
miR-126	miR-375	0.86
miR-127-3p	miR-375	0.91
miR-133a	miR-375	0.87
miR-139-5p	miR-375	0.90
miR-145	miR-375	0.89
miR-15b	miR-375	0.93
miR-17	miR-375	0.89
miR-186	miR-375	0.85
miR-192	miR-375	0.97
miR-193a-5p	miR-375	0.89
miR-193b	miR-375	0.94
miR-197	miR-375	0.93
miR-19b	miR-375	0.95
miR-204	miR-375	0.96
miR-20a	miR-375	0.98
miR-20b	miR-375	0.90
miR-21	miR-375	0.94
miR-223	miR-375	0.90
miR-24	miR-375	0.92
miR-26a	miR-375	0.87
miR-30b	miR-375	0.91
miR-30c	miR-375	0.92
miR-324-3p	miR-375	0.96
miR-331-3p	miR-375	0.89
miR-106a	miR-376a	0.87
miR-127-3p	miR-376a	0.94
miR-139-3p	miR-376a	0.91
miR-140-3p	miR-376a	0.89
miR-140-5p	miR-376a	0.89
miR-145	miR-376a	0.86
miR-193b	miR-376a	0.88
miR-199a-3p	miR-376a	0.88
miR-21	miR-376a	0.89
miR-223	miR-376a	0.86
miR-25	miR-376a	0.95
miR-28-3p	miR-376a	0.91
miR-328	miR-376a	0.88
miR-191	miR-411	0.87
miR-103	miR-423-5p	0.90
miR-106b	miR-423-5p	0.89
miR-127-3p	miR-423-5p	0.89
miR-133a	miR-423-5p	0.92
miR-139-3p	miR-423-5p	0.86
miR-140-5p	miR-423-5p	0.93
miR-142-3p	miR-423-5p	0.90
miR-145	miR-423-5p	0.98
miR-15b	miR-423-5p	0.90

miR-17	miR-423-5p	0.96
miR-181a	miR-423-5p	0.89
miR-185	miR-423-5p	0.89
miR-186	miR-423-5p	0.95
miR-192	miR-423-5p	0.91
miR-193a-5p	miR-423-5p	0.93
miR-193b	miR-423-5p	0.89
miR-197	miR-423-5p	0.94
miR-19a	miR-423-5p	0.96
miR-19b	miR-423-5p	0.89
miR-204	miR-423-5p	0.88
miR-21	miR-423-5p	0.89
miR-223	miR-423-5p	0.94
miR-24	miR-423-5p	0.92
miR-28-3p	miR-423-5p	0.88
miR-30b	miR-423-5p	0.94
miR-30c	miR-423-5p	0.95
miR-324-3p	miR-423-5p	0.91
miR-328	miR-423-5p	0.97
miR-331-3p	miR-423-5p	0.93
miR-345	miR-423-5p	0.86
miR-370	miR-423-5p	0.89
miR-375	miR-423-5p	0.90
miR-106a	miR-425	0.99
miR-106b	miR-425	0.88
miR-126	miR-425	0.97
miR-127-3p	miR-425	0.93
miR-133a	miR-425	0.87
miR-139-3p	miR-425	0.89
miR-139-5p	miR-425	0.96
miR-140-5p	miR-425	0.86
miR-145	miR-425	0.90
miR-146a	miR-425	0.89
miR-15b	miR-425	0.90
miR-16	miR-425	0.89
miR-17	miR-425	0.91
miR-186	miR-425	0.85
miR-192	miR-425	0.92
miR-193b	miR-425	0.98
miR-197	miR-425	0.94
miR-19b	miR-425	0.96
miR-204	miR-425	0.96
miR-20a	miR-425	0.88
miR-20b	miR-425	0.93
miR-21	miR-425	0.97
miR-222	miR-425	0.88
miR-223	miR-425	0.95
miR-24	miR-425	0.98
miR-25	miR-425	0.96
miR-26a	miR-425	0.88
miR-28-3p	miR-425	0.89
miR-28-5p	miR-425	0.86

miR-30b	miR-425	0.91
miR-30c	miR-425	0.92
miR-320	miR-425	0.88
miR-324-3p	miR-425	0.93
miR-328	miR-425	0.87
miR-331-3p	miR-425	0.89
miR-342-3p	miR-425	0.91
miR-375	miR-425	0.91
miR-376a	miR-425	0.86
let-7d	miR-451	0.88
miR-106b	miR-451	0.87
miR-122	miR-451	0.99
miR-139-5p	miR-451	0.88
miR-192	miR-451	0.88
miR-19b	miR-451	0.86
miR-204	miR-451	0.89
miR-20a	miR-451	0.92
miR-20b	miR-451	0.90
miR-26a	miR-451	0.94
miR-324-3p	miR-451	0.86
miR-339-3p	miR-451	0.86
miR-374a	miR-451	0.90
miR-375	miR-451	0.92
miR-143	miR-483-5p	0.97
miR-146a	miR-483-5p	0.87
miR-191	miR-483-5p	0.86
miR-222	miR-483-5p	0.85
miR-320	miR-483-5p	0.90
miR-106a	miR-484	0.89
miR-126	miR-484	0.91
miR-140-5p	miR-484	0.92
miR-143	miR-484	0.90
miR-145	miR-484	0.85
miR-146a	miR-484	0.96
miR-150	miR-484	0.89
miR-17	miR-484	0.89
miR-181a	miR-484	0.89
miR-186	miR-484	0.86
miR-191	miR-484	0.87
miR-197	miR-484	0.86
miR-222	miR-484	0.99
miR-223	miR-484	0.89
miR-24	miR-484	0.89
miR-25	miR-484	0.86
miR-28-3p	miR-484	0.93
miR-28-5p	miR-484	0.88
miR-30c	miR-484	0.86
miR-320	miR-484	0.99
miR-328	miR-484	0.88
miR-330-3p	miR-484	0.89
miR-342-3p	miR-484	0.91
miR-425	miR-484	0.86

miR-483-5p	miR-484	0.91
miR-101	miR-486-3p	0.93
miR-138	miR-486-3p	0.98
miR-198	miR-486-3p	0.96
miR-331-5p	miR-486-3p	0.94
let-7d	miR-486-5p	0.91
miR-106a	miR-486-5p	0.88
miR-126	miR-486-5p	0.91
miR-139-5p	miR-486-5p	0.91
miR-146b-5p	miR-486-5p	0.90
miR-150	miR-486-5p	0.89
miR-193b	miR-486-5p	0.90
miR-197	miR-486-5p	0.88
miR-19b	miR-486-5p	0.92
miR-204	miR-486-5p	0.92
miR-223	miR-486-5p	0.85
miR-24	miR-486-5p	0.90
miR-29b	miR-486-5p	0.85
miR-30b	miR-486-5p	0.85
miR-324-3p	miR-486-5p	0.85
miR-342-3p	miR-486-5p	0.91
miR-425	miR-486-5p	0.89
miR-103	miR-491-5p	0.92
miR-106b	miR-491-5p	0.86
miR-140-3p	miR-491-5p	0.92
miR-148a	miR-491-5p	0.94
miR-221	miR-491-5p	0.92
miR-370	miR-491-5p	0.93
miR-374b	miR-491-5p	0.97
miR-27a	miR-494	0.97
miR-27a	miR-495	0.95
miR-494	miR-495	0.97
miR-335	miR-500	0.90
miR-361-5p	miR-500	0.93
miR-1	miR-501-5p	0.95
miR-101	miR-502-3p	0.98
miR-138	miR-502-3p	0.90
miR-198	miR-502-3p	0.87
miR-331-5p	miR-502-3p	1.00
miR-486-3p	miR-502-3p	0.94
miR-101	miR-517a	0.99
miR-138	miR-517a	0.92
miR-331-5p	miR-517a	0.97
miR-486-3p	miR-517a	0.92
miR-502-3p	miR-517a	0.97
miR-101	miR-519e	0.99
miR-138	miR-519e	0.90
miR-198	miR-519e	0.87
miR-331-5p	miR-519e	1.00
miR-486-3p	miR-519e	0.94
miR-502-3p	miR-519e	1.00
miR-517a	miR-519e	0.97

miR-1	miR-520d-5p	0.90
miR-23a	miR-520d-5p	0.96
let-7e	miR-532-3p	0.94
miR-142-3p	miR-532-3p	0.95
miR-17	miR-532-3p	0.87
miR-185	miR-532-3p	0.96
miR-186	miR-532-3p	0.86
miR-19a	miR-532-3p	0.90
miR-30b	miR-532-3p	0.88
miR-30c	miR-532-3p	0.86
miR-331-3p	miR-532-3p	0.91
miR-345	miR-532-3p	0.94
miR-339-3p	miR-532-5p	0.86
miR-103	miR-539	0.92
miR-106b	miR-539	0.86
miR-140-3p	miR-539	0.93
miR-148a	miR-539	0.93
miR-221	miR-539	0.92
miR-370	miR-539	0.93
miR-374b	miR-539	0.97
miR-491-5p	miR-539	1.00
miR-454	miR-548a-3p	0.89
miR-146b-5p	miR-574-3p	0.99
miR-150	miR-574-3p	0.96
miR-29b	miR-574-3p	0.98
miR-342-3p	miR-574-3p	0.93
miR-486-5p	miR-574-3p	0.92
miR-103	miR-598	0.93
miR-106b	miR-598	0.88
miR-140-3p	miR-598	0.92
miR-148a	miR-598	0.98
miR-193a-5p	miR-598	0.86
miR-221	miR-598	0.95
miR-370	miR-598	0.97
miR-374b	miR-598	0.99
miR-491-5p	miR-598	0.98
miR-539	miR-598	0.98
miR-101	miR-625	0.98
miR-138	miR-625	0.89
miR-198	miR-625	0.88
miR-331-5p	miR-625	1.00
miR-486-3p	miR-625	0.94
miR-502-3p	miR-625	1.00
miR-517a	miR-625	0.96
miR-519e	miR-625	1.00
miR-129-3p	miR-629	0.94
miR-28-5p	miR-629	0.93
miR-330-3p	miR-629	0.89
miR-10b	miR-636	0.90
miR-1	miR-652	0.90
miR-100	miR-660	0.90
miR-146a	miR-660	0.88

miR-15b	miR-660	0.91
miR-16	miR-660	0.85
miR-186	miR-660	0.88
miR-197	miR-660	0.89
miR-19a	miR-660	0.86
miR-19b	miR-660	0.87
miR-204	miR-660	0.86
miR-30c	miR-660	0.88
miR-324-3p	miR-660	0.90
miR-330-3p	miR-660	0.86
let-7b	miR-885-5p	0.92
let-7d	miR-885-5p	0.95
miR-122	miR-885-5p	0.88
miR-204	miR-885-5p	0.86
miR-451	miR-885-5p	0.87
miR-486-5p	miR-885-5p	0.93
let-7e	miR-886-3p	0.90
miR-142-3p	miR-886-3p	0.93
miR-17	miR-886-3p	0.86
miR-185	miR-886-3p	0.90
miR-186	miR-886-3p	0.88
miR-197	miR-886-3p	0.85
miR-19a	miR-886-3p	0.90
miR-223	miR-886-3p	0.86
miR-30b	miR-886-3p	0.92
miR-30c	miR-886-3p	0.87
miR-331-3p	miR-886-3p	0.87
miR-345	miR-886-3p	0.90
miR-532-3p	miR-886-3p	0.95
let-7d	miR-886-5p	0.91
miR-103	miR-886-5p	0.91
miR-106a	miR-886-5p	0.88
miR-106b	miR-886-5p	0.95
miR-122	miR-886-5p	0.86
miR-126	miR-886-5p	0.88
miR-127-3p	miR-886-5p	0.92
miR-133a	miR-886-5p	0.88
miR-139-5p	miR-886-5p	0.93
miR-145	miR-886-5p	0.90
miR-15b	miR-886-5p	0.89
miR-17	miR-886-5p	0.89
miR-192	miR-886-5p	0.96
miR-193a-5p	miR-886-5p	0.87
miR-193b	miR-886-5p	0.96
miR-197	miR-886-5p	0.92
miR-19b	miR-886-5p	0.95
miR-204	miR-886-5p	0.96
miR-20a	miR-886-5p	0.98
miR-20b	miR-886-5p	0.89
miR-21	miR-886-5p	0.95
miR-223	miR-886-5p	0.93
miR-24	miR-886-5p	0.94

miR-25	miR-886-5p	0.86
miR-26a	miR-886-5p	0.87
miR-30b	miR-886-5p	0.94
miR-30c	miR-886-5p	0.91
miR-324-3p	miR-886-5p	0.94
miR-328	miR-886-5p	0.85
miR-331-3p	miR-886-5p	0.89
miR-375	miR-886-5p	0.99
miR-423-5p	miR-886-5p	0.90
miR-425	miR-886-5p	0.92
miR-451	miR-886-5p	0.89
miR-486-5p	miR-886-5p	0.86
miR-101	miR-9	0.89
miR-10b	miR-9	0.86
miR-129-3p	miR-9	0.92
miR-198	miR-9	0.86
miR-224	miR-9	0.86
miR-331-5p	miR-9	0.94
miR-486-3p	miR-9	0.87
miR-502-3p	miR-9	0.95
miR-517a	miR-9	0.86
miR-519e	miR-9	0.94
miR-625	miR-9	0.95
let-7e	miR-92a	0.92
miR-106a	miR-92a	0.94
miR-106b	miR-92a	0.86
miR-126	miR-92a	0.96
miR-127-3p	miR-92a	0.87
miR-133a	miR-92a	0.93
miR-139-5p	miR-92a	0.87
miR-140-5p	miR-92a	0.93
miR-145	miR-92a	0.95
miR-146a	miR-92a	0.91
miR-15b	miR-92a	0.89
miR-16	miR-92a	0.89
miR-17	miR-92a	0.99
miR-181a	miR-92a	0.89
miR-185	miR-92a	0.87
miR-186	miR-92a	0.95
miR-192	miR-92a	0.91
miR-193a-5p	miR-92a	0.90
miR-193b	miR-92a	0.95
miR-197	miR-92a	0.98
miR-19a	miR-92a	0.93
miR-19b	miR-92a	0.96
miR-204	miR-92a	0.95
miR-20a	miR-92a	0.85
miR-21	miR-92a	0.91
miR-222	miR-92a	0.92
miR-223	miR-92a	0.99
miR-24	miR-92a	0.98
miR-25	miR-92a	0.88

miR-28-3p	miR-92a	0.89
miR-30b	miR-92a	0.98
miR-30c	miR-92a	0.97
miR-320	miR-92a	0.91
miR-324-3p	miR-92a	0.92
miR-328	miR-92a	0.94
miR-331-3p	miR-92a	0.97
miR-342-3p	miR-92a	0.90
miR-345	miR-92a	0.87
miR-375	miR-92a	0.89
miR-423-5p	miR-92a	0.93
miR-425	miR-92a	0.94
miR-484	miR-92a	0.90
miR-486-5p	miR-92a	0.89
miR-532-3p	miR-92a	0.87
miR-886-3p	miR-92a	0.90
miR-886-5p	miR-92a	0.92
let-7e	miR-93	0.87
miR-142-3p	miR-93	0.88
miR-181a	miR-93	0.94
miR-328	miR-93	0.85
miR-345	miR-93	0.85
miR-532-3p	miR-93	0.86
miR-106a	miR-99b	0.89
miR-125a-5p	miR-99b	0.91
miR-127-3p	miR-99b	0.90
miR-139-3p	miR-99b	0.93
miR-139-5p	miR-99b	0.86
miR-20b	miR-99b	0.91
miR-21	miR-99b	0.91
miR-25	miR-99b	0.90
miR-26a	miR-99b	0.90
miR-323-3p	miR-99b	0.91
miR-324-3p	miR-99b	0.86
miR-425	miR-99b	0.91

Online Table IV. miRNA network topology values

ID	Node degree	Clustering coefficients	Betweenness centrality	Clusters
miR-197	46	0.6087	294.6777	1
miR-223	46	0.61739	220.8167	1
miR-92a	46	0.6	2.50E+02	1
miR-17	45	0.61414	223.9829	1
miR-30c	45	0.61616	275.9978	1
miR-145	43	0.6268	232.1945	1
miR-24	43	0.67331	137.052	1
miR-425	43	0.6124	922.3542	1
miR-204	42	0.60511	474.7849	1
miR-193b	41	0.66463	149.1595	1
miR-19b	41	0.65732	314.4007	1
miR-30b	41	0.64024	240.3027	1
miR-106a	40	0.6359	727.1196	1
miR-331-3p	40	0.65	165.9824	1
miR-324-3p	39	0.68961	207.2898	1
miR-126	38	0.66999	498.0567	1
miR-192	38	0.69417	210.0613	1
miR-328	38	0.6074	3.84E+02	1
miR-186	37	0.63063	171.1418	1
miR-21	36	0.73492	74.2007	1
miR-886-5p	36	0.71746	1.49E+02	1
miR-106b	35	0.61849	546.8299	1
miR-133a	34	0.74866	82.9921	1
miR-375	34	0.74153	113.1221	1
miR-423-5p	34	0.70232	60.4924	1
miR-127-3p	33	0.76894	46.5204	1
miR-15b	32	0.71573	178.5295	1
miR-103	31	0.60215	398.927	3
miR-140-5p	31	0.70968	79.5007	1
miR-193a-5p	31	0.66452	157.2165	1
miR-25	30	0.72184	166.843	1
miR-19a	29	0.67488	78.6356	1
miR-20a	28	0.7619	67.0426	1
miR-222	28	0.61111	762.8777	6
miR-139-5p	27	0.70655	103.4128	1
miR-146a	27	0.61254	385.378	6
miR-28-3p	27	0.74359	88.0549	1
miR-320	27	0.57835	5.96E+02	6
miR-484	26	0.58769	5.49E+02	6
miR-139-3p	24	0.69928	161.9982	1
miR-20b	22	0.71429	146.5313	1
miR-486-5p	21	0.57143	347.002	4
let-7e	20	0.62632	474.383	1
miR-181a	20	0.64211	106.4101	1
miR-342-3p	20	0.58421	316.9526	4
miR-16	19	0.87719	12.605	1
miR-185	17	0.85294	5.948	1

let-7d	16	0.59167	262.511	7
miR-451	16	0.61667	440.929	9
miR-142-3p	15	0.77143	15.0857	1
miR-370	15	0.59048	8.61E+01	3
miR-26a	14	0.62637	152.4076	0
miR-345	14	0.76923	13.9276	1
miR-376a	14	0.78022	52.9869	1
miR-886-3p	14	0.87912	2.37E+00	1
miR-532-3p	13	0.82051	9.24E+00	1
miR-28-5p	12	0.51515	2613.8708	11
miR-660	12	0.68182	7.81E+02	0
miR-99b	12	0.62121	1.38E+02	12
miR-122	11	0.74545	13.0798	9
miR-150	11	0.58182	93.0062	4
miR-374b	11	0.76364	17.2521	3
miR-9	11	0.47273	2.43E+03	2
miR-140-3p	10	0.53333	39.3779	3
miR-221	10	0.8	9.8385	3
miR-598	10	0.84444	7.06E+00	3
miR-331-5p	9	0.91667	2.63E+01	2
miR-486-3p	9	0.91667	26.3214	2
miR-491-5p	9	0.91667	3.4064	3
miR-502-3p	9	0.91667	2.63E+01	2
miR-519e	9	0.91667	2.63E+01	2
miR-539	9	0.91667	3.41E+00	3
miR-625	9	0.91667	2.63E+01	2
miR-101	8	0.96429	25.75	2
miR-138	8	0.92857	0.57143	2
miR-148a	8	0.96429	0.44653	3
miR-330-3p	8	0.46429	1.03E+03	11
miR-517a	8	0.96429	25.75	2
miR-191	7	0.42857	438.6377	5
miR-198	7	0.95238	25.75	2
miR-199a-3p	7	0.66667	11.8802	1
miR-146b-5p	6	0.8	41.3623	4
miR-374a	6	0.6	30.7824	9
miR-483-5p	6	0.86667	3.6722	5
miR-885-5p	6	0.6	36.4249	7
miR-93	6	0.6	2.10E+00	1
miR-129-3p	5	0.3	3478	0
miR-143	5	0.9	3.0345	5
miR-29b	5	1	0	4
miR-574-3p	5	1	0.00E+00	4
miR-1	4	0	866	10
miR-195	3	1	0	1
miR-323-3p	3	1	0.00E+00	12
miR-339-3p	3	0.33333	2.20E+02	0
miR-629	3	1	0.00E+00	11
let-7b	2	1	0	7
let-7c	2	0	220	8
miR-100	2	0	436	8
miR-10b	2	0	220	0

miR-125a-5p	2	1	0	12
miR-27a	2	1	0	13
miR-301a	2	0	220	0
miR-335	2	1	0.00E+00	14
miR-361-5p	2	1	0.00E+00	14
miR-494	2	1	0	13
miR-495	2	1	0	13
miR-500	2	1	0.00E+00	14
miR-520d-5p	2	0	220	0
miR-15a	1	0	0	8
miR-224	1	0	0	2
miR-23a	1	0	0	0
miR-29c	1	0	0.00E+00	5
miR-365	1	0	0	0
miR-411	1	0	0	5
miR-454	1	0	0	0
miR-501-5p	1	0	0	10
miR-532-5p	1	0	0.00E+00	0
miR-548a-3p	1	0	0.00E+00	0
miR-636	1	0	0.00E+00	0
miR-652	1	0	0	10

Online Figure I. Properties of miRNA co-expression network. A) Probability density distribution of Pearson correlation coefficients (PCC). Interestingly, there were very few negative correlations. **B)** Number of nodes in the miRNA network and **C)** number of edges in the co-expression network as a function of PCC. As PCC values increased, weak edges were removed, while node number remained constant. **D)** At larger PCC values, the network became modular as evidenced by the decreasing but large clustering coefficient. **E)** Network information flow described by the average eigenvector centrality. **F)** Scale-free architecture of the miRNA co-expression network dominated by a small number of central nodes attached to a large number of loosely connected miRNAs. These topological features are consistent with the general behavior of biological networks and topologies detected in protein-protein interaction collections such as STRING.

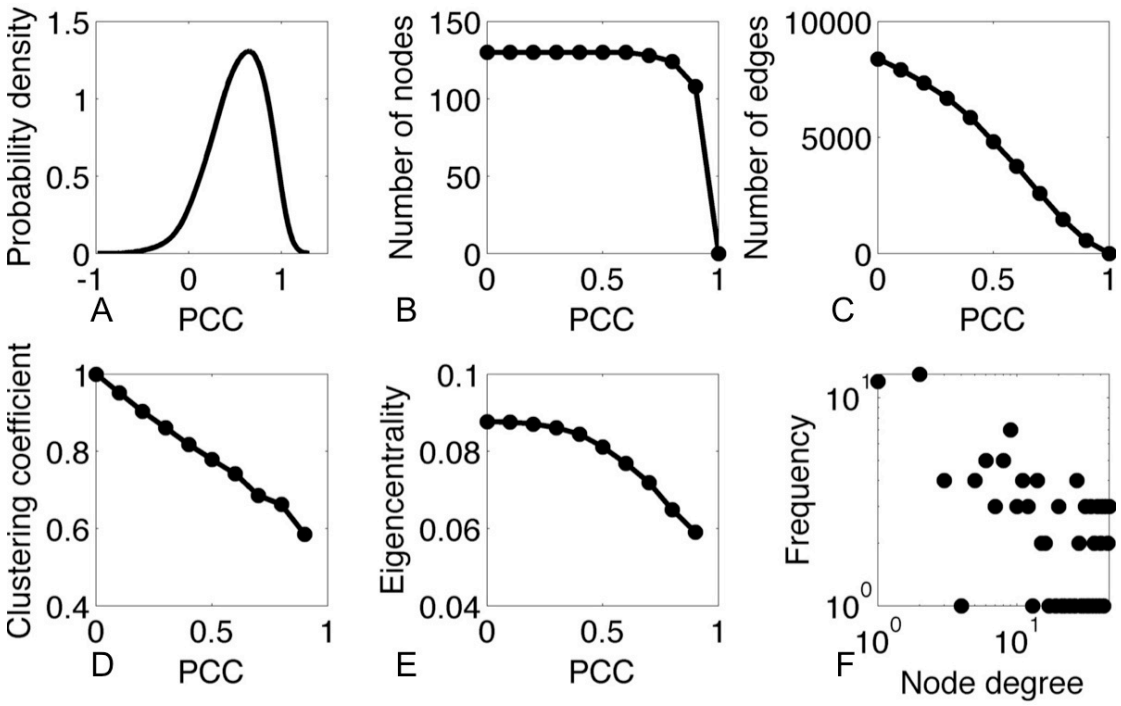

Online Figure II. miRNA co-expression network inferred from microarray experiments for 13 differentially expressed and topologically unique miRNAs. Of the 30 differentially expressed miRNAs (blue), 13 miRNAs (red) were selected by probing their topological properties in a co-expression network, inferred using Pearson Correlation Coefficients (PCC), as opposed to individual over- or under-expression. Significant miRNAs co-expressions are represented as network edges.

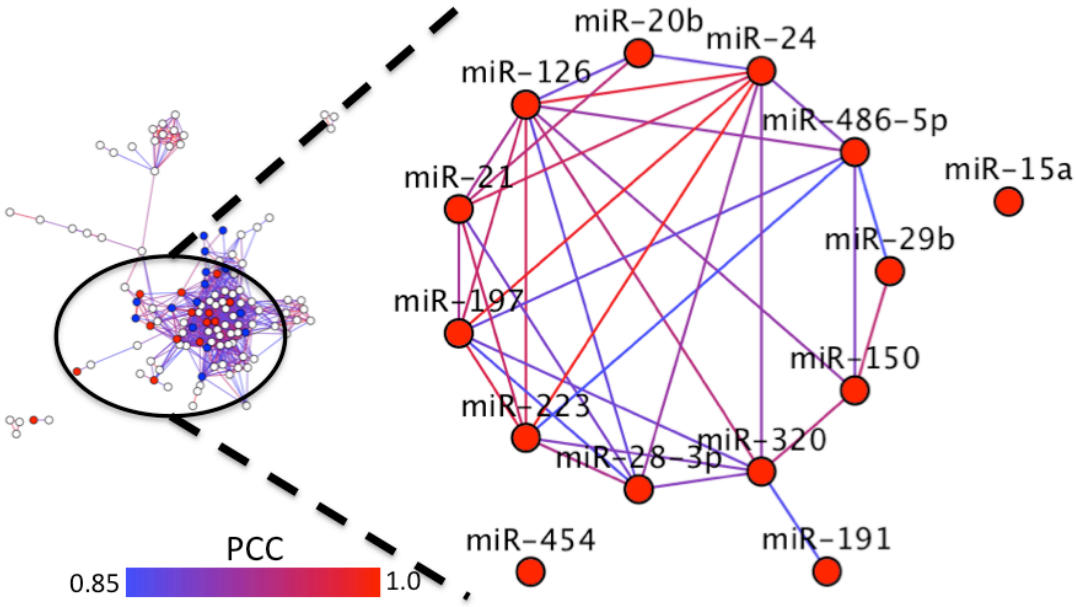

Online Figure III. MiRNA networks. A) Differential network structure between 13 miRNAs in controls (n=91) and manifest DM (n=56). Nodes represent individual miRNAs and edges (links) represent the extent of expression similarity measured using the Context likelihood of relatedness algorithm. Control (13 nodes, 25 links) and DM (13 nodes, 19 links) networks shared only 10 links. The disease state was characterized by substantial edge rewiring (miR-15a). **B)** Differential topology of control and DM networks. The control network (green bars) was characterized by a larger node degree, clustering coefficient and eigenvector centrality than the one in DM (red bars).

A.

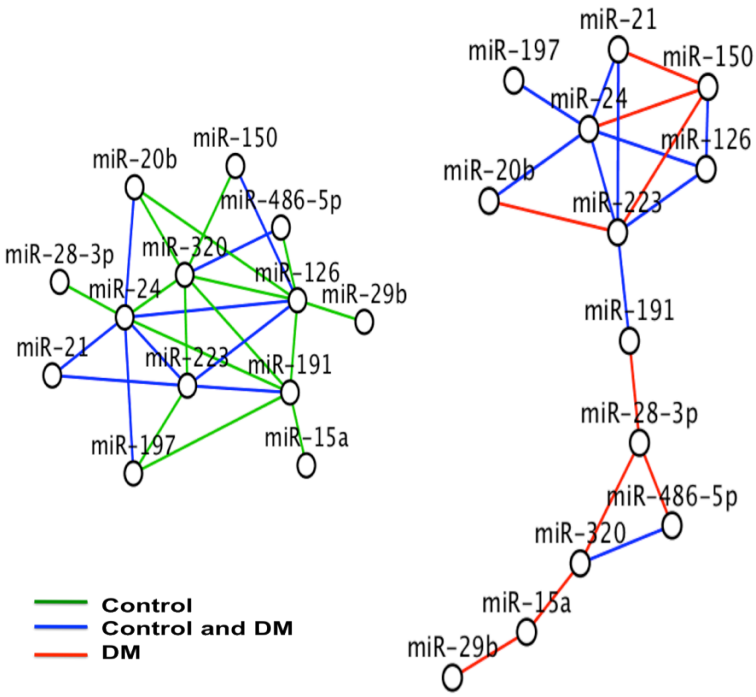

B.

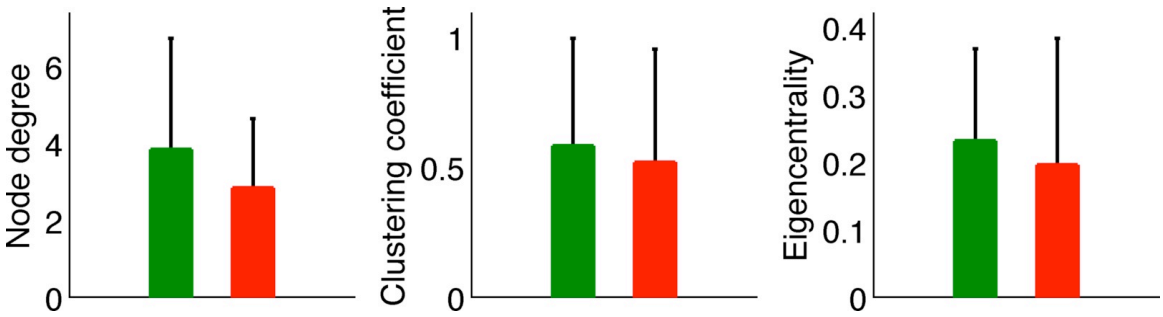

Online Figure IV. High glucose leads to selective decrease in miRNA content in endothelial derived apoptotic bodies. The effect of increased glucose on the miRNA content of endothelial derived apoptotic bodies were assessed using qPCR. miR-454 was used as a normalization control. Data shown are of four independent experiments and presented as means SEM, * $p<0.05$